Preprint
Please cite as:
Fiorillo F., Petitta M., Preziosi E,. Rusi S., Esposito L., Tallini M. (2015): *Long-term trend and fluctuations of karst spring discharge in a Mediterranean area (central-southern Italy).* Environ. Earth. Sci., 74/1, 153-172, Doi https://10.1007/s12665-014-3946-6

Long term trend and fluctuations of karst spring discharge in a Mediterranean area (Central-Southern Italy)

Francesco Fiorillo[1], Marco Petitta[2], Elisabetta Preziosi[3], Sergio Rusi[4], Marco Tallini[5]

[1] Dipartimento di Scienze e Tecnologie, University of Sannio, Via dei Mulini 59/A, 82100 Benevento, Italy e-mail: francesco.fiorillo@unisannio.it
[2] Dipartimento di Scienze della Terra, University "La Sapienza", 00185 Rome, Italy e-mail: marco.petitta@uniroma1.it
[3] CNR–IRSA, National Research Council–Water Research Institute, Via Salaria km 29,300, PB 10, 00015 Monterotondo, Rome, Italy e-mail: elisabetta.preziosi@cnr.it
[4] Dipartimento di Ingegneria e Geologia, University "G. d'Annunzio", Via dei Vestini, 30 66013 Chieti, Italy e-mail s.rusi@unich.it
[5] Dipartimento di Ingegneria Civile, Edile-Architettura e Ambientale-Centro di Ricerca e Formazione in Ingegneria Sismica, Università dell'Aquila, 67100 L'Aquila, Italy e-mail: marco.tallini@univaq.it

Abstract

Karst springs in central-southern Italy are largely exploited for the human consumption since the Roman Times and currently feed some tens of millions inhabitants with tap water of high quality. Unlike other karst springs, they provide a steady rate during the year with a low monthly variation. However, the effects of climate changes are being strongly perceived in central and southern Italy as in the rest of the Mediterranean basin, and groundwater is obviously also affected. In this paper we analyse the discharge time series of some important karst springs in the region, evaluating the trends and fluctuations in relation to rainfall regime, on a yearly time scale. The aim is to evaluate the response of these large karst aquifers in the Mediterranean area to the recharge input variation. The role of the North Atlantic Oscillation has also been considered. Trends and fluctuations have been highlighted by *n*-years moving average and transforming the time series by the Rescaled Adjusted Partial Sum. The results show that a drop in the discharge has occurred since 1987, with reductions ranging from 15% up to 30%, although this negative trend is now possibly attenuating or even reversing. As a final remark, the spring discharge of the large karst aquifers in Central-Southern Italy can be assumed as a robust indicator for climate changes as it integrates the effects of precipitation and temperature variation in time and space.

Keywords

groundwater, karst aquifer, NAO, RAPS, climate changes, time series

1. Introduction

Wide areas of central-southern Italy are fed by large karst springs, firstly tapped by Roman aqueducts to supply towns throughout the Roman Times. During the last century, these karst springs have been largely exploited to supply big cities such as Rome and Naples, and numerous other towns and villages. Currently, in many regions of Italy, karst springs provide large amount of the drinking water, and supply some tens of millions of people. These springs are fed by wide fractured and karstified aquifers, which originate from high carbonate massifs, generally hydraulically isolated by thick flysch sequences or other non-karstic impervious terrains along their boundaries. Locally, due to the typical Mediterranean climate, the recharge is concentrated prevalently during autumn and winter; as a consequence, karst aquifers discharge water throughout the hydrological year, primarily in response to this climate regime, and also to the geological-geomorphological setting and karst conditions (Fiorillo, 2009). The recent geological evolution of these aquifers frequently did not allow a development of mature karst in the discharge zones, causing a relatively steady regimen in respect to the classical mature karst springs. In these conditions, spring discharge is influenced both by the seasonal recharge cycle and by a multi-annual "memory" effect due to the reservoir storage. Consequently, these wide karst systems act as large natural reservoirs of water, and karst spring discharges reflect periods of poor or abundant precipitations, as well as long term climate change (Fiorillo and Guadagno, 2010; 2012).

The climatic change observed worldwide indicates that the regime of these springs is changing, and that the main consequence in the Mediterranean area is a drop in the spring discharge due to a decrease in rainfall and an increase in temperature. A decrease of annual and winter rainfall is observed in Southern Italy since the 1980s, whereas summer rainfalls present a positive trend (Caloiero et al., 2011). A similar situation was observed also in central Italy by Romano and Preziosi (2013). Fiorillo et al. (2007) analyzed the long-spring discharge series of the Serino springs (Campania), and highlighted the drop in discharge after 1986. Ducci and Tranfaglia (2008) estimated a decrease of 30% of the average infiltration in Campania region, within the present climate scenario, due to rainfall drop and temperature increase. Fiorillo and Guadagno (2012) analysed long time series of karst spring discharge in Campania region and found that each annual mean spring discharge series shows similar characteristics, with periods of low and high flow common to all the springs. Nanni and Rusi (2003) found a direct correlation between the thickness of the seasonally accumulated snowpack and the discharge of the main springs in the Majella

massif. Petitta and Tallini (2002) verified the influence of natural changes on spring discharge in the Gran Sasso aquifer, coupled with human induced alteration due to tunneling drainage. Preziosi and Romano (2013) found that karst spring discharge in central Italy show consistent signals of the effects of climate changes with declines of about 20% in the period 1938-2007.

In this study the discharge time series of some important karst springs in Central and Southern Italy (Fig. 1) have been considered, evaluating the trends and fluctuations in relation to rainfall, based on a yearly time scale, to evaluate their response to recharge input, considering possible relationships with climatic parameters at the Mediterranean scale. The role of North Atlantic Oscillation (NAO) has also been considered, comparing its influence at the annual and multi-years time scale.

The large karst springs of Tirino (Gran Sasso massif), Acqua Marcia (Simbruini mountains), Verde (Maiella massif), Serino and Caposele (Picentini mountains) have been analysed, annual rainfall at several rain gauges and NAO index as well. For this purpose, the annual mean values have been standardised, and correlations have been found. Trends and fluctuations have been highlighted by *n*-years moving average and transforming the time series by the Rescaled Adjusted Partial Sum (Garbrecht and Fernandez, 1994).

2. Hydrogeological features

The whole study area has been interested by the evolution of the Central Apennine chain, developed with time from west to east (Fig. 1). After the Tyrrhenian margin, showing narrow coastal plains filled up by transitional Quaternary deposits, the peri-Tyrrhenian volcanic belt is related to the recent extensional tectonic phases. The main domain is the Meso-Cenozoic Central-Southern Carbonate Apennines, which during Upper Miocene have been displaced, fragmented and overthrusted with an imbricate geometry toward ENE. Along the front of the thrust belt, the foredeep basin is represented by silicoclastic deposits, partially overthrusted towards the Adriatic margin, showing wide coastal plains filled up mostly by continental and marine deposits. The Quaternary and recent evolution, leaded by the extensional tectonic and erosion, enhanced the development of intramontane plains and alluvial valleys among the carbonate ridges.

The Central-Southern Apennines are characterized by wide carbonate ridges (Fig. 1) representing the main aquifers, whose groundwater is drained at their borders where low-permeability deposits outcrop by large flow springs with steady regimen. These lithotypes are synorogenetic

silicoclastic sediments and Plio-Quaternary deposits (alluvial, lacustrine, detrital origin) which filled the intramontane plains or river valleys. While the silicoclastic sediments (no-flow boundaries) act as real aquicludes, the continental deposits form multilayer aquifer/aquitard systems, causing springs to flow and allowing seepage through the more permeable layers of the plain (e.g., gravel, sand and travertines). Downthrown carbonates can host deeper groundwater flow in confined aquifers, causing locally artesian conditions.

In the carbonate Central Apennines, groundwater is supplied by large recharge areas corresponding to the main ridges, feeding about 80 springs and streambed springs whose mean discharge range between 1 m^3/s and 18 m^3/s (Fig. 1). High rainfall rates and snowmelt supply a large amount of recharge waters, while developed surface and epikarst systems, including endorheic basins, enhance the infiltration rate. As a result, recharge can reach values higher than 1000 mm/y. The hydraulic gradient is generally lower than 1% and low-permeability bedrock corresponds to the Triassic dolomites.

The recent evolution of internal Apennine areas, associated with extensional tectonic movements, was causing the fast deposition of very thick continental depositional sequences (Cavinato and De Celles, 1999), affecting groundwater flow in the surrounding fractured carbonate aquifers and hindering the development of a mature karst network in the discharge areas of the regional aquifer. Indeed, sedimentation rate and tectonic activity tend to alter the base level of the fractured aquifer, contrary to what usually happens in karst regions (Petitta, 2009; Petitta et al., 2014). It follows that, in the Apennine carbonate aquifers, groundwater flow is concentrated towards springs, showing a modulate response to seasonal recharge. Consequently, high storage of these large and deep aquifers determines steady baseflow from springs (Petitta 2009; Desiderio et al., 2012). Indeed, karst behavior and large conduit flow are limited in this domain, feeding few springs having a real “karst” discharge regimen. This hydrogeological situation has a double advantage: the karst development in recharge area ensures high-rate infiltration and consequently huge renewable resources, while the flow concentrated in fracture network feeds steady regimen springs in the discharge areas.

Table 1 and 2 summarize the main hydrogeological/hydrological characteristics and statistics of the springs and of the meteorological station analyzed in the four study areas discussed in this paper and described more in details in the following paragraphs.

2.1 Gran Sasso aquifer

The Gran Sasso Carbonate Aquifer (GSCA) is located in the Abruzzi region (central Italy), at the northern limit of the Meso-Cenozoic carbonate platform lithofacies of Central Apennines, being a partitioned, fissured and karstified aquifer (Fig. 1). The GSCA hydrogeological setting is briefly highlighted, referring to previous studies for an in-depth analysis, including local and regional hydrogeological features (Amoruso et al., 2012; Amoruso et al., 2014; Petitta and Tallini, 2002; Petitta and Tallini, 2003; Scozzafava and Tallini, 2001; Tallini et al. 2006), hydrochemistry and isotope hydrology (Adinolfi Falcone et al., 2008; Barbieri et al., 2005; Tallini et al., 2013; Tallini et al., 2014), and also earthquake hydrology (Adinolfi Falcone et al., 2012; Amoruso et al., 2011).

The GSCA is a fractured aquifer (Fig. 2), represented by an outcrop of 700 km^2 of Meso-Cenozoic carbonate rocks that are more than 2000 m thick, with well-defined boundaries represented by Miocene terrigenous aquitard along its northern boundary marked by a regional thrust (T in Fig. 2) and by Quaternary clastic aquitard, along its southern side. The aquifer total discharge from its springs amounts to more than 18 m^3/s. With a mean hydraulic gradient of 5‰, it is locally compartmentalized by faults that act as groundwater divides and/or low-permeability heterogeneities. The GSCA is recharged by a net infiltration of over 800 mm/y, to be compared with an annual average rainfall of approximately 1200 mm/y (Scozzafava and Tallini, 2001). A preferential recharge zone is located in the central region of the ridge and corresponds to the endhoreic basin of Campo Imperatore (elevation 1650 m a.s.l.). In the saturated zone, dual velocity of groundwater flow has been inferred (Adinolfi Falcone et al., 2008), according with the hydraulic conductivity values evaluated for main fractures (10^{-4} m/s) and for fracture network in carbonate rocks (10^{-7} to 10^{-6} m/s; Monjoie, 1980). Extensional Quaternary tectonic is prevalent in the southern sector and governs the intra-montane basin evolution and its filling through continental clastic deposits, such as the L'Aquila Plain and Campo Imperatore (Cavinato and De Celles, 1999).

The major springs, characterized by high and steady discharge rates (0.5-7 m^3/s), are located at the boundaries of the aquifer (discharge zones) and lie along no-flow and seepage limits defined by aquitards. Water table levels close to these springs are steady with constant head conditions (Wang and Anderson, 1982) at the aquifer boundaries. Seasonal fluctuations of the water table lead to higher water levels in late spring and early summer and lower levels in autumn/winter.

Main springs have been divided into six groups, based on groundwater flow and hydrochemical characteristics (Barbieri et al., 2005; Petitta and Tallini, 2002; Tallini et al., 2013; Tallini et al.,

2014). The springs located on the Gran Sasso northern side (total discharge: 2 m^3/s), are fed by the overflow aquifer along the no flow boundary thrust T (Fig. 2). Some springs located at SW boundary of the aquifer near L'Aquila city (total discharge: 1 m^3/s) are probably fed by fast-circulating karst-type aquifer (Amoruso et al., 2012; Barbieri et al., 2005; Tallini et al., 2013), while the springs located in L'Aquila Plain are due to the mixing of shallow and regional groundwater (Petitta and Tallini, 2003).

A portion of the water table has been partially drained since the 1980s because of the excavation of an underground laboratory (UL) and two highway tunnels (Adinolfi Falcone et al., 2008) (Fig. 2). The two highway tunnels intercept the regional groundwater flow at about 980 m a.s.l. (causing a transient decline of the water table after the tunnel boring) and are tapped for drinking use on both sides. Groundwater drainage is captured by two pairs of 5-km long channels, located under the highway tunnels (Fig. 2). The UL of the Italian National Institute of Nuclear Physics (INFN) shows an additional groundwater drainage partially driven to the main drainage channels, while the other half is directly driven to the northern exit of the tunnels. The hydraulic gradient from the UL to the highway tunnels has been enhanced by the drainage, overtaking the value of 50% at local scale (about 300 m from the tunnels). This drainage therefore corresponds to the shallow circulating groundwater which has low salinity and short residence time, from which all the others evolve. The groundwater flow can be considered gravity driven from the aquifer core to the springs located at its boundaries, as demonstrated by the increase of temperature and salinity along the flowpaths (Adinolfi Falcone et al. 2008).

The main groundwater flow is directed to the south-eastern boundary, where the Tirino River springs (about 13 m^3/s, more than 60% of the entire aquifer discharge) are located (Fig. 2), due to the outcropping of regional water table at low elevations along the Gran Sasso ESE boundary (Petitta and Tallini, 2002).

The Tirino River is totally fed by groundwater flow, coming from the main springs of Presciano and Capodacqua, because of negligible runoff contribution. The gauging station of Bussi (Tirino River at Madonnina), located downstream of the two main springs, is recording the hydrometric level since 1937, but only since 1970 a correlation curve allows to evaluate the river discharge, which corresponds to the sum of the spring discharge of Presciano, Capodacqua and other minor streambed springs. Consequently, the gauging station on Tirino River can be used as hydrograph of a spring group of a carbonate fractured/karstified aquifer, with negligible contribution by runoff.

The mean long-term discharge of the Tirino River calculated at Bussi gauging station is about 6.7 m^3/s, a steady value scarcely affected by seasonal significant changes (less than 10%), because it corresponds to the base level of the groundwater flow of the regional GSCA aquifer.

Maximum long-term discharge at the Tirino River appears usually in spring (April-May), followed by a tiny exhaustion phase recorded in July-August. The spring long-term regime is not really representing the discharge changes with time, because of the shift of the high- and low-discharge period in single years. In fact, in the studied period 1970-2013, the extreme monthly discharge values felt for each year in different months, testifying a seasonal regime without fixed recharge/discharge periods; this characteristics is resumed in Fig. 3, where the occurrence of maximum and minimum values in different years are plotted. The dataset highlights that extreme values are recorded at least one time for each month, with highest occurrence of peaks in October-December and lowest in July-September; otherwise, the minimum discharges are more frequent in summer and rare in spring.

In respect to this long-term stable regime, Tirino spring yearly discharge has a wider variability, showing a standard deviation of 1.6 m^3/s. Annual data clearly show a decrease trend since '70s, but two external factors significantly influenced the natural discharge with time. In the '80 the drainage from the highway tunnels affected the discharge of all GSCA springs, including the Tirino ones; the decrease amount has not been calculated, but the transient effect of the drainage is probably exhausted after 5-10 years; this situation does not affect pluriannual changes, because of the steady amount of tunnel drainage. A second interference on groundwater flow was due to the April 6th 2009 L'Aquila Earthquake (Amoruso et al., 2011; Adinolfi Falcone et al., 2012; Galassi et al., 2014), which clearly caused a discharge increase along the boundaries of the aquifer, due to pore-pressure effect and to fracture cleaning effect; consequently, discharge since 2009 shows higher values with respect to the expected natural changes. The response of the flow system in the Tirino River Valley to the cited earthquake is directly confirmed by a symmetric water table rise in the monitoring wells located in the valley (Adinolfi Falcone et al., 2012), highlighting the increase in discharge of this portion of the GSCA. A simplified estimation of the additional flow rate reaching the Tirino Valley, based on the water table rise (up to 2.5 m), on the regional hydraulic gradient (5‰) and on the groundwater flow section of the Tirino Valley (about 2500 m wide, with an effective porosity of about 5%), evidenced an expected increase of discharge in Tirino River springs of about 1.5 m^3/s, which exactly corresponds to the discharge increase recorded in April 2009-December 2013 period (from 5.4 to 6.9 m^3/s).

2.2 Maiella aquifer

The structure of the Majella (273 km^2) is hydraulically isolated on the surface on all sides (Fig. 4), while in depth it is limited on three fronts (E, S and W). The northernmost front of the structure extends below the Mio-Pleistocene terrigenous units of the Pescara valley, and does not exclude its hydraulic continuity in this direction.

Within the Majella structure the following hydrogeological complexes can be recognized (Fig. 4): – a hydrogeological complex of Jurassic-Paleocene limestone characterized by high permeability due to karst and fissuring; – an aquiclude of the Bolognano Formation consisting of marly limestone and marlstone; – a hydrogeological complex of calcarenites of the Bolognano Formation characterized by variable permeability, decreasing northward, caused by fracturing and porosity; – an aquiclude of terrigenous and evaporitic formations consisting of clay, marl and marly clay; – a hydrogeological complex of highly permeable continental detritus.

The aquifer has a total spring discharge of about 8 m^3/s and is recharged by a net infiltration of over 900 mm/y (Nanni and Rusi, 2001, 2003) vs. an average rainfall of about 1450 mm/y. The recharge of the Majella hydrostucture takes place exclusively by precipitation (snow and rain), without any water yield from the adjacent structures. The perched aquifers are recharged both by melting snow and by rainwater. The snow-covered zones at high altitude are characterized by extensive plains, with less intense karstic phenomena (Agostini & Rossi, 1992) and the greater abundance of detritus. This influences recharge, with two consequences: 1) it reduces infiltration in winter and early spring, in turn reflecting on the basal emergence hydrographs, unaffected in these periods; 2) it causes marked spring and summer infiltration due to the slow melting of snow in zones with elevated infiltration capacity. The effect of the melting snow can be clearly seen both qualitatively and quantitatively (Nanni and Rusi, 2003).

The remarkable ramification of the superficial circuits due to fissuring and karst is demonstrated by the presence of over 240 springs. The recharge circuits are very rapid, with delays of less than 15 days between the rainy or melting event and the relative discharge increment. The rapid circuits are highlighted by the ever-present seasonal thermal signal, the limited turnover times and the emptying capacity (Nanni and Rusi, 2003). Within this general trend, however, it is possible to characterize various kinds of circuits depending on whether the spring comes from the hydrogeological complex of the Cretaceous-Paleocene limestones or from the extended detrital covering.

The basal springs of the hydrostucture (Fig. 4) are located in the eastern and northern slopes, with average discharges varying from 0.6 to 3.5 m^3/s. All the registered parameters indicate that they are recharged by circuits pertaining to a single aquifer, whose dimensions, volumetric capacity and depth increase northward.

In fact the more southern springs, even if they involve elevated volumes of water (average discharge 0.6 - 1 m^3/s), are characterised by active circulation in which the delay between recharge event and discharge increase was estimated at 15 - 30 days. In particular, the analysis of the hydrographs established the presence of karstic conduits overlapping with fissured circuits, giving delay times of 15 days for the former and 1 or 2 months for the latter (Nanni and Rusi 2003). The active circulation is confirmed by the inverse correlation between electrical conductivity and discharge, due to the poor mixing with deep waters and dilution of nearly all the chemical-physical parameters.

The central northern springs (including Verde spring) involve considerable water volumes (average discharge 0.6 – 3.5 m^3/s), and are characterised by slow circulation zones. The increased discharge of the springs here, closely correlated to snow melting, is caused by piezometric lifting in the emergence zone. This phenomenon is in turn due to a transfer of pressure resulting from a rapid increment of hydraulic charge in the central area of the basal aquifer, due to a very fast infiltration of melted snow. This kind of circulation is confirmed also by the constancy of chemical-physical parameters (Nanni and Rusi, 2003) and by the elevated turnover time (4 – 6 years).

The northern part of the basal aquifer emerges from the Lavino spring at Decontra through a N - S system of faults that allows the water to rise through the argillaceous complex and flysch sequences (Fig. 4). The circulation of the Lavino spring is more complex than the other emergences because of the crossing of evaporitic units, with consequent mineralization, and the superposition of a shallow circuit and basal circuit.

A single basal aquifer was recognised with maximum extension and elevated hydrodynamic characteristics in the central part of the hydrostructure. The hydrogeologic balance (Nanni and Rusi, 2003) excludes both the presence of water yields from the borderland structures, in particular from the Porrara M., or the presence of great flows towards the buried northern continuation of the structure.

The Verde Spring (its waters are used for about 25% for drinking and about 75% for hydroelectric purposes) is located in the lowest point of the contact between calcareous aquifer and argillaceous aquitard. The contact is masked to a slope breccias from which emerges the spring.

The gauging station of Verde (Verde River at Fara S. Martino, Table 1), located downstream of the spring, is recording the hydrometric level since 1938 with two missing periods (1943-1945 and 1981-1985).

The mean long-term discharge of the Verde spring (Table 1) is about 3,2 m^3/s. Maximum long-term discharge appears usually in late-spring (Jun), followed by a long exhaustion phase recorded until September-October. Annual data (Fig. 9) clearly show a decrease trend since the late '80s.

The continuous monitoring of the chemical-physical parameters (Nanni and Rusi, 2003) shows a constant trend. The temperature is constantly 8.5 °C, while the electrical conductivity varies only between 220 – 250 μS/cm.

The spring is characterized by constant discharge in autumn and winter with a maximum value in late Spring due to the melting of snow during the previous 15-30 days; the very intense storms not influence the hydrographs. The fluctuation of the discharge and the correspondent scarce variations in the chemical-physical parameters are due to a fast circulation in the unsaturated zone which is slow in the saturated zone. Therefore, in Spring there is a fast reconstitution (15-30 days) of the dynamic resources of the aquifer by the waters of the melting of snow and this phenomenon increases by a transfer of pressure, the discharge of the springs.

2.3 Simbruini aquifer

The Simbruini aquifer (Fig. 5) is the northern part of a larger hydrostructure which includes the Monti Ernici, Monte Cairo and Monti delle Mainarde and extends over 1780 km^2 delivering a mean annual discharge of 48-52 m^3/s through several springs and seepage along rivers (Boni et al., 1986). The effective infiltration was estimated 850 mm/a out of 1330 mm of annual precipitation. Schematically it can be described as an anticline oriented NW-SE, mainly formed by a very thick carbonate platform sequence (Latium-Abruzzo sequence), mainly consisting of limestones, ranging from Trias to Paleocene, unconformably overlaid by calcarenitic limestones and silicoclastic foredeep sediments of Miocene age (Sani et al., 2004; Calamita et al., 2008). The Triassic part of the sequence is composed by dolomites and dolomitic limestone, outcropping in the central part of the area, which is supposed to act as the impervious bed of the aquifer. This structure overthrust the flysch sequences (lower Messinian) of the Roveto Valley on the East; the main tectonic elements of apenninic direction (NW-SE) are supposed to drive the groundwater flow. Simbruini Mountains feed a series of important springs (Fig. 5), including the seepage along of the upper Aniene river (6.5 m^3/s), the Liri valley springs on the East (3.2-3.3 m^3/s) and the Acqua

Marcia group (mean discharge 5.4-5.7 m^3/s, Boni et al. 1986; ACEA, 2001). Surface and underground karst features are highly developed and some of the springs (e.g. the Inferniglio and the Pertuso springs) are fed through karstic conduits, with important submerged passages, partially explored for about 6 km of length (Mecchia et al 2003). Huge endorheic areas (Arcinazzo, Camposecco) cover part of the structure favoring high rates of effective infiltration.

Acqua Marcia (named after the console Marcio Re who realized the first aqueduct to derive these springs to the city of Rome during the Roman Republic time, in 79 b.C.) is composed by a number of springs located between 322 and 329 m a.s.l. at the northern end of the structure, outcropping at the boundary with the Miocene turbiditic sequences. The recharge area occupies the north-western part of the hydrostructure for 250 km^2. The water can be classified bicarbonate–earth-alkaline type HCO_3-Ca-Mg, with a mean temperature of 9.5-10 °C (ACEA, 2001). The mean discharge is about 5.5 m^3/s, 4.5 m^3/s being diverted to the city of Rome, providing about 20-25% of the total supply for this city. Monthly discharge data are available from 1938 to 2007 (ACEA, 2001).

2.4 Picentini aquifers (Terminio and Cervialto massifs)

The northern sector of Picentini mountains (Figures 1 and 6) is characterized by several massifs, and the ground-elevation reaches 1809 and 1806 m a.s.l. in correspondence of Mt. Cervialto and Terminio peaks, respectively. In general, these massifs are characterized by high slope angles, connected to Quaternary tectonic uplift, which has caused several fault-scarp in the carbonaceous rocks, actually showing a slope angle around 35°-45°.

Locally a series of limestone and limestone-dolomite (Late Triassic-Miocene) outcrops, characterized by a thickness ranging between 2500 and 3000 m. Along the northern and eastern sectors, these massifs are tectonically overlapped on the terrigenous and impermeable deposits (Fig. 6), constituting argillaceous complexes (Paleocene) and flysch sequences (Miocene). More specific geological insight of the outcropping areas can be found in Parotto and Praturlon (2004) and related literature, and Geological Map of Italy, 1:50.000 scale (ISPRA, 2009).

These massifs are characterized by wide endorheic areas (Fig. 6), which have an important role in the recharge processes. The largest are the Piana del Dragone (55,1 km^2) and Piano Laceno for Terminio and Cervialto massif, respectively. The origin of these endorheic zones is connected to tectonic activity during upper Pliocene-Pleistocene, which has caused a general uplift by direct faults, and formation of graben zones; during the following continental environment (Pleistocene-

Olocene), karst processes have transformed these zones in endorheic ones, allowing the complete absorption of runoff, and the formation of seasonal lakes (Fiorillo et al., 2014).

Pyroclastic deposits of Somma-Vesuvius activity cover the Picentini mountains, with thickness up to several meters along gentle slopes, and only few decimeters along steep slopes. The pyroclastic cover is generally composed of several irregular, ashy pumiceous layers, intercalated with weathered ash deposits; while the pumice layers are composed of coarse material (sand and gravel), the interlayered remoulded and weathered ash deposits are finer materials (sand and silt, with low clay fraction).

The powerful springs of these massifs are shown in Fig. 6. The Serino group is located in the valley of the Sabato River, along the north-western boundary of the Picentini massif and is formed by the Acquaro-Pelosi springs (377–380 m a.s.l.) and the Urciuoli spring (330 m a.s.l.). These springs are fed by the Terminio massif (Civita, 1969; Fiorillo et al., 2007), with an overall mean annual discharge of 2.25 m^3/s. Roman aqueducts (first century A.D.) were supplied by these springs and the Urciuoli spring was re-tapped between 1885 and 1888 by the Serino aqueduct, which is comprised of a gravity channel followed by a system of pressured conduits that is used to supply water to the Naples area. Additionally, the Aquaro and Pelosi springs were also re-tapped in 1934 by the Serino aqueduct.

The Caposele group is formed by the Sanità spring (417 m a.s.l.), which is located at the head of the Sele river basin along the north-eastern boundary of the Picentini Mountains. This spring, which is primarily fed by the Cervialto mountain (Celico and Civita, 1976), has a mean annual discharge of 3.96 m^3/s. The spring was tapped in 1920 by the Pugliese aqueduct, which passes through the Sele-Ofanto divide via a tunnel and supplies the Puglia region with water.

The long spring discharge measurements and the relation to climate variable have been analyzed by Fiorillo and Guadagno (2012), and the hydraulic aquifer behavior during dry periods has been described by Fiorillo (2009) and Fiorillo et al. (2012).

As other typical areas of Italian peninsula, the monthly rainfall reaches a maximum during November and a minimum in July. The pattern of potential evapotranspiration computed using the method described by Thornthwaite and Mather (1957) was found to be almost completely opposite to that of rainfall, reaching a maximum in July and a minimum in December–February. The maximum discharge of Serino and Caposele springs occurred several months after the maximum rainfall, whereas the minimum discharge occurred during the wettest period. In

particular, Caposele spring has almost the opposite trend respect to the precipitations: the minimum discharge occurs during the maximum of precipitation, and viceversa.

For the Terminio and Cervialto massifs a detailed estimation of afflux and recharge have been carried out on annual (Allocca et al., 2014; Fiorillo et al., 2014)) and daily scale model (Fiorillo et al., 2014), and table 3 shows some hydrological parameters computed in GIS environment.

Data series used in this study are shown in table 1; generally, a daily frequency of the discharge measurements have been carried out since 1962, whereas previous measurements had a frequency twice or three times a month; in particular, for Serino springs data are available since 1887 (Fiorillo et al., 2007). The data time series is not completely continuous; however, breaks in the data series are generally not longer than a few months, and are filled by simple interpolation.

3. Material and methods

Daily precipitation and daily minimum and maximum temperature data were available from the National or Regional Hydrographic Services. They were aggregated at both the annual (hydrologic year, September through August) and monthly time step.

Discharge data of the springs were available from the Hydrographic Service or from the water supply companies (Acqua Marcia from ACEA S.p.A.; Caposele from Acquedotto Pugliese S.p.A.; Serino from ARIN S.p.A.) aggregated at the monthly and annual (hydrologic year November through October) time step.

To compare the different spring discharge time series, the annual mean values (November through October), Q_i, have been standardized, Q_s, by the following:

$$Q_s = \frac{Q_i - \mu}{\sigma} \qquad \textbf{(1)}$$

where μ and σ are the mean and the standard deviation of the series, respectively.

In the same way, annual rainfall values (September through August), P_i, have been transformed in the standardized values, P_s, by the following:

$$P_s = \frac{P_i - \mu}{\sigma} \qquad \textbf{(2)}$$

where μ and σ are the mean and the standard deviation of the series, respectively.

The transformed values are dimensionless; in particular, positive/negative values of Q_s or P_s indicate values above/below the mean of Q_i and P_i, respectively. The transformation in standardized values allows to compare karst springs characterized by different discharge

magnitude; independently from trends and ciclicity existing in the time series, standardized plot simply allows to distinguish periods of lower than average / higher than average flow, and highlights the extreme values (Fiorillo and Guadagno, 2012). Besides, if values of a time series can approximate a normal distribution, the standardized values are directly linked to the probability of occurrence.

Spring discharge and rainfall standardized time series have been compared to the North Atlantic Oscillation (NAO) (Walker, 1924; Walker and Bliss 1932) index (Hurrell, 1995). The NAO is a well known atmospheric phenomenon in the North Atlantic Ocean, and concerns the fluctuations in the difference of atmospheric pressure at sea level between the *Icelandic low* (a semi-permanent centre of low atmospheric pressure found between Iceland and southern Greenland) and the *Azores high* (the large subtropical semi-permanent centre of high atmospheric pressure typically found south of the Azores). Through fluctuations in the strength of the *Icelandic low* and the *Azores high*, NAO controls the strength and direction of the westerly winds and storm tracks across the North Atlantic. Although the NAO occurs in all seasons, during winter it is particularly dominant, and therefore the focus of this information is in the December through March period. The sea level pressure (SLP) averaged over the winter is considered; in particular, the variability of the NAO depends on the difference between the mean winter SLP at Gibraltar (or Azores, or Lisbon) and the SLP over Iceland. Strong positive phases of the NAO tend to be associated with above-average precipitation over northern Europe and Scandinavia in winter, and below-average precipitation over southern and central Europe; opposite patterns of precipitation anomalies are typically observed during strong negative phases of the NAO (Walker and Bliss 1932; Hurrell 1995). The principal component (PC) time series of the leading Emperical Orthogonal Function (EOF) of the December through March SLP anomalies over the Atlantic sector (20-80N, 90W-40E) serves as an alternative index (Hurrell 1995; 2003). These data series are available at NCARS (2014) and allow for a direct comparison with spring discharge and rainfall data series. In particular, as the NAO index seems to be related to the amount of precipitation over the Mediterranean area especially during the winter period (Lamb and Peppler, 1987; Massei et al., 2009; Romano and Preziosi, 2013), which coincides with the peak of precipitation over the Italian peninsula, the annual mean spring discharge and annual rainfall with NAO index have been compared.

The progressive accumulation of standardized values provides the Rescaled Adjusted Partial Sums (RAPS) transformation of data series. Specifically, RAPS of the time series $\{Y_t\}$ are defined as follows:

$$RAPS_k = X_k = \sum_{t=1}^{k} \frac{Y_t - \mu}{\sigma_Y} \qquad \textbf{(3)}$$

where μ is sample mean, σ_Y is the standard deviation, n is the number of values in the time series, k is counter limit of the current summation. The plot of the RAPS versus time is the visualisation of the trends and fluctuations of Y_t, and highlights trends, shifts, data clustering, irregular fluctuations, and periodicities in the record (Garbrecht and Fernandez, 1994). In particular, decreasing patterns in the RAPS are the result of mostly below-average Y_t values, whereas increasing patterns are the result of periods of mostly above-average Y_t values.

Autocorrelation of the annual mean spring discharge and annual effective rainfall series were conducted to determine if there is any link between consecutive values. In statistic, the autocorrelation of a random process describes the correlation between values of the process at different points in time, as a function of the two times or of the time difference. Let X_t be the value of the process at time t, whereas t may be an integer for a discrete-time process or a real number for a continuous-time process. If X_t has mean μ and variance σ^2, which are supposed to be returned as an unbiased estimate, then the autocorrelation is defined as (Benjamin and Cornell, 1960):

$$r_{xx}(k) = \frac{1}{(n-k)\sigma^2} \sum_{t=1}^{n-k} (X_t - \mu)(X_{t+k} - \mu) \qquad \textbf{(4)}$$

where n is the number of samples and k is any positive integer such as $k < n$.

For k=0 the r_{xx} value is 1. For k=1 the r_{xx} value expresses the link between two consecutive values of the series, and it tends to $r_{xx} \approx 0$ in a pure random series. Higher the link between consecutive values of series and slower $r_{xx} \rightarrow 0$ when k>0; this behaviour highlights the memory effect of a time series, where each value depends on the antecedent value and indicates the inertia in responding to external factors (Fiorillo and Doglioni, 2010).

4. Data analysis and discussion

Central and Southern Italy have a typical Mediterranean climate, characterized by dry and warm summers, and wet periods occurring during the fall, winter and spring. Monthly rainfall reaches its highest annual peak during November-December, while the minimum occurs during July-August (Fig. 7). The Mediterranean signal appear clearly in all climate stations (Fig.7a), where the monthly distribution of rainfall is similar; a higher autumn-winter concentration of rainfall occurs in the southern climate station (Serino). The Mediterranean climate amplifies the concentration of the

distribution of the effective rainfall during November-February period (Fig. 7b), and generally cause a long period of soil moisture deficit during the long and dry summer.

In the highly-elevated zones (above 1000 m a.s.l.) snow can accumulate for several weeks during winter, providing a time-shift of the recharge processes along springtime. Above 1500-2000 m a.s.l., particularly for Gran Sasso and Maiella karst massifs, snowy accumulation can occur up to late spring season, amplifying the shift between precipitation and recharge processes. The combined effect of increasing evapotranspiration and decreasing rainfall towards the summer season results in the negligible effective rainfall after April until September; therefore, in Mediterranean climate, the rainfall that occurs up to March–April of each hydrological year have a strong control in recharging karst aquifers, and subsequent rainfall, period from May up to September-October, generally does not contribute to the aquifer recharge (Fiorillo, 2009).

Hydrographs of karst springs (Fig. 8) primarily reflect the amount of cumulative rainfall that has occurred from the beginning of the rainy season, and a strict correlation between annual rainfall and annual mean spring discharges (Fig. 7 and 8) frequently exists (Fiorillo and Guadagno, 2010, 2012). However, large springs may also depend on a longer cumulative rainfall, and the role of antecedent annual rainfall could influence the discharge of the following hydrological year (Fiorillo, 2009). The distribution of monthly mean discharges and their percentage variation are shown in Figure 8, where largest springs have lower intra-annual variation.

Figure 9 shows the discharge standardized series of all the springs and rainfall (Tables 1 and 2 provide characteristics of the springs and rain gauges), compared with the NAO, which is believed one of the factors controlling the climate conditions in the Mediterranean area (Lamb and Peppler, 1987; Massei et al., 2009; Lopez—Moreno et al., 2008; Lopez-Moreno et al., 2011; Romano and Preziosi, 2013).

The results of the linear correlation are shown in Tables 4 and 5. It appears that the NAO has a strong control on the spring discharge, as expected, with the lowest value at the Tirino spring.

Negative values of the NAO index are generally correlated to positive values of standardized annual spring discharge, and viceversa. In detail, it is possible to observe that after 1986/87 all series clearly show a decrease in discharge values, which has been reversed during the most recent years. The lower values of 1949 and 2002 are well marked in all series, as well as other intense droughts of 1943, 1946, 1975 and of the recent period 2007-2008.

The highest discharge values of the Picentini springs (Caposele and Serino) were induced by the 23 November 1980 Irpinia earthquake (Ms=6.9); in particular this earthquake caused an anomalous

increase in spring discharge (Celico, 1981; Cotecchia and Salvemini, 1981), with maximum values of 7.32 m^3/s (19 January 1981), and 3.6 m^3/s (18 January 1981), being observed for the Caposele and Serino springs, respectively. The Tirino spring series is affected by a similar effect, recorded after the 6 April 2009 L'Aquila earthquake (Ms=6.3); this anomalous increase is due both to the short-term pore-pressure propagation and to the fracture cleaning effect having mid-term consequences. The Tirino spring annual discharge rose of more than 30%, in respect with the previous years, reaching a peak of 7.4 m^3/s in 2011 in respect with the discharge of 5.2 m^3/s recorded in 2008 (Amoruso et al., 2011; Adinolfi Falcone et al., 2012; Galassi et al., 2014; Petitta et al., 2014).

For all the four karst systems, a rain gauge located on the western side of the aquifer, which well records the precipitation pattern coming prevalently from Atlantic direction, has been considered (Fiorillo, 2009; Allocca et al., 2014). Obviously, each annual rainfall data series cannot reflect the recharge amount on a specified aquifer, because of the variability of the precipitation over each massif; the standardised annual rainfall time series only would indicate the succession of wet and dry hydrological years, which have a control on the annual mean spring discharge. Rainfall time series are shown in Figure 9b, and should reflect the pattern of the annual mean spring discharge (Fig 9a). However, the annual rainfall data series appear scattered in respect to spring discharge data series; then, the wet and dry periods, which induce high and low flow periods in the spring discharge series, appear more difficult to define. However, the lowest values of the rainfall cause the most intense droughts in the spring discharge series, as found especially for Picentini springs (Fiorillo and Guadagno, 2012). Looking at table 6, a significant correlation exists between annual rainfall and spring discharge, especially for Serino and Caposele springs. However, some rain gauges appear uncorrelated with spring discharge data series, and more complex relationship could exist. In any cases, the annual mean spring discharge are better correlated with the NAO index than with the annual rainfall. This could be associated to the higher spatial variability of the precipitation, whereas spring discharge appears a more "robust" indicator of the inflow, because it expresses the climate characteristic of a wider area integrating the recharge in time and space, as expected.

In the Tiber basin, the correlation between the annual standardized precipitation index and the winter NAO index was estimated R=−0.36 by Romano and Preziosi (2013), and a bit stronger with the winter precipitation (-0.54). De Vita et al. (2012) found similar results in the correlation between NAO and the annual precipitation in Campania, and Caposele spring discharge.

Considering that the spring discharge is affected not only by annual recharge but also by a memory effect, the correlation has also been evaluated between time series of several *n*-years moving average, where higher correlation coefficients are obtained (Tab 7 and 8). However, in these cases, the time series tend to show a similar cyclicity and the high-self dependence could fail the meaning of correlations.

Autocorrelation of the annual mean spring discharge and annual effective rainfall series have been calculated to determine if there is any link between consecutive values (Fig. 10a). For a value of k=1, the coefficient of autocorrelation, r(k), is still significant for all springs, especially for Tirino and Acqua Marcia springs. This parameter highlights the memory effect of data series and could explain the limited correlation with annual rainfall. The NAO data series appear uncorrelated, annual rainfall data series as well (Figure 10b). Fiorillo (2009) discussed on the tendency of annual mean spring discharge values to "bunch" together, especially for large springs.

The tendency of data clustering, connected to memory effect in data series, appears clearly in the RAPS plot (figure 11). The time series of RAPS for the annual mean spring discharge (Figure 11a) shows a positive trend during 1934-1942, 1951-1974 (a break occurs during the drought of 1968) and 1977-1981 periods. Negative trends occurred during 1943-1950 period; since 1987 RAPS presents negative trends, interrupted only during 1999, 2006 and more recent years. These general trends of RAPS of annual mean spring discharge appear controlled by the trend of RAPS of the NAO; the strong positive trend during the sixties and negative trend during the eighties-nineties are well evident.

RAPS of the annual rainfall (Figure 11b) shows similar trends of the spring discharge, proving that the annual rainfall series control the spring discharge. However, some differences exist between the two types of series; in particular, the negative trend during the eighties-nineties appears attenuated in the RAPS of rainfall, indicating that the drop of spring discharge in the same period has to be connected also to other causes. A possible explanation could be that, after 1986, the relationship between rainfall/spring discharge has changed, and aquifers became less sensitive to the rainfall. In other words, an amount of rainfall does not contribute to the spring discharge as in the past, and a possible explanation of this new response would be the global warming which increases the evapotranspiration processes (Fiorillo and Guadagno, 2012). Fiorillo and Guadagno (2010) have shown that local temperature has been increasing since the 1980s, as well as worldwide data (MOHC, 2010), and confirmed by other studies in Italy (e.g. Brunetti et al., 2006).

As regards the examined springs, it is apparent that a drop in the discharge has occurred since 1987, with reductions ranging from 15% (Caposele) up to 30% (Tirino). A negative trend of the annual mean spring discharge has been found since 1964 for the Fontane de Vaucluse karst spring (France) by the RAPS method (Bonacci, 2007), based on 1878-2004 period. During the recent decades, no-drop in the annual rainfall has been observed in the Fontane de Vaucluse spring catchment (Bonacci ,2007), indicating the probable influence of the temperature increase observed since the eighties. After 2009-2010 the available data concerns only NAO index, Tirino spring and Subiaco S.S. rainfall station. In spite of the scarce data, it is possible to observe that the negative trend for the NAO index that started in the eighties, is now possibly diminishing or reversing, as well as that of the rainfall and the discharge.

5. Conclusion

Some representative springs fed by carbonate fractured karst aquifers in Central-Southern Italy have been studied to evaluate their response to recharge input, considering possible relationships with climatic parameters at the continental scale. The analyzed springs are characterized by a prevalent slow flow component, without discharge peaks during meteoric inflow, and the higher the annual mean discharge, the lower the discharge variability through the hydrological year (Figures 8).

This typical regimen of the basal karst aquifers of the Apennine range, can be sought in the huge extension and the high mean elevation of recharge areas, which result in high baseflow rates and significant memory effect, able to modulate the high autumn-winter recharge and to limit the decrease of discharge during the long dry Mediterranean season. Besides, the dense fracture network, superimposed to the locally developed karst conduits, is able to slow down the groundwater flow and to regularly distribute it over time, typical of the diffuse karst system.

The high mean elevation of the recharge areas, especially of those draining towards the Adriatic Sea (East), up to 3000 m a.s.l., which receives a large part of the winter precipitation as snowfall, contributes to modulate the discharge with time, decreasing the winter and spring picks and increasing the summer baseflow.

In this framework, pluriannual changes can be analyzed in detail, showing variations attributable to climate influence at a larger scale than the aquifer ones.

In general, the regimen of the analyzed springs is very similar although not identical. Observed variations among them can be attributed to local different geological-hydrogeological asset, the

diverse fracture and karstification degree, the different amount of distribution of liquid and solid precipitation, which is function of the ground elevation distribution of spring catchments and of the orographic conditions. The different size of the spring catchment area also has a fundamental role in controlling the spring regime.

The availability of multidecadal time series (up to one century long) allowed the analysis of the relationships among spring discharges and the NAO: the existence of a linear correlation clearly demonstrates that the NAO has a strong control on the spring discharge, evidencing a continental scale effect on aquifer recharge/discharge, more evident than local precipitation/discharge relationship for large springs. Consequently, the trend of spring discharge of karst aquifers in Central-Southern Italy can be assumed as a robust climate indicator. Minor correlation values as recorded for Tirino spring would be due to significant influence of memory effect, which can be highlighted by comparison by the RAPS.

The time series of RAPS for the annual mean spring discharges follow the trend of RAPS of the NAO; in fact, the strong positive trend during the sixties and negative trend during the eighties-nineties are both well evident.

Similarly, RAPS of the annual rainfall shows a similar trend to that of the springs discharge, proving that the annual rainfall influences the spring discharge. Some differences exist between the two types of series: the negative trend during the eighties-nineties appears attenuated in the RAPS of rainfall, indicating that the drop of spring discharge in the same period may be due not simply to a precipitation decrease, but possibly to different rainfall time distribution and/or to temperature changes; additional investigation on this topic can further clarify the causes of this evident response. Nevertheless, it can be stated that, after 1986, the relationship between rainfall/spring discharge has changed, and aquifers appear to be less sensitive to the rainfall amount in respect with the previous period. The results of this study clearly show the need to looking for a more comprehensive approach to individuate the causes of pluriannual discharge changes and drop, recorded in springs in karst Apennine aquifers in the last century.

A wide-scale approach has been found useful to demonstrate that NAO has a strong control on the discharge of the karst springs, specially at the multi-yearly time scale, individuating a clear diffuse negative trend of the discharge more pronounced after 1986-1987. This long positive phase of NAO, and the consequent poor spring discharge, appears broken since 2008/09, when strong negative values of the NAO occurred, inducing a return of wet years and a consequent spring discharge recover.

References

ACEA, 2001. Proposta di area di salvaguardia per le sorgenti dell'Acquamarcia (Groundwater Safeguard Protection Areas Proposal for the Exploitation System of the Acquamarcia Spring), Hydrogeological Report. S13PR0020 (in Italian).

Adinolfi Falcone R, Carucci V, Falgiani A, Manetta M, Parisse B, Petitta M, Rusi S, Spizzico M, Tallini M (2012) Changes on groundwater flow and hydrochemistry of the Gran Sasso carbonate aquifer due to the 2009 L'Aquila earthquake. Ital J Geosci (Boll Soc Geol It) 131: 459-474. doi: 10.3301/IJG.2011.34

Adinolfi Falcone R, Falgiani A, Parisse B, Petitta M, Spizzico M, Tallini M (2008) Chemical and isotopic ($\delta^{18}O‰$, $\delta^{2}H‰$, $\delta^{13}C‰$, ^{222}Rn) multi-tracing for groundwater conceptual model of carbonate aquifer (Gran Sasso INFN underground laboratory – central Italy). Journal of Hydrology 357: 368-388.

Agostini S, Rossi MA (1992-93) Il carsismo della Majella (Abruzzo). Le grotte d'Italia 16: 31-40.

Amoruso A, Crescentini L, Petitta M, Rusi S, Tallini M (2011) Impact of the April 6, 2009 L'Aquila earthquake on groundwater flow in the Gran Sasso carbonate aquifer, Central Italy. Hydrological Processes 25: 1754-1764. doi: 10.1002/hyp.7933

Amoruso A, Crescentini L, Petitta M, Tallini M (2012) Parsimonious recharge/discharge modeling in carbonate fractured aquifers: the groundwater flow in the Gran Sasso aquifer (Central Italy). Journal of Hydrology 476: 136–146. http://dx.doi.org/10.1016/j.jhydrol.2012.10.026.

Amoruso A, Crescentini L, Petitta M, Tallini M (2014) Correlation between groundwater flow and deformation in the fractured carbonate Gran Sasso aquifer (INFN underground laboratories, Central Italy). Water Resour. Res., 50, 1-19, doi:10.1002/2013WR014491.

Allocca V, Manna F, De Vita P (2014) Estimating annual groundwater recharge coefficient for karst aquifers of the southern Apennines (Italy). Hydrol. Earth Syst. Sci., 18, 803–817

Barbieri M, Boschetti T, Petitta M, Tallini M (2005) Stable isotopes (^{2}H, ^{18}O and $^{87}Sr/^{86}Sr$) and hydrochemistry monitoring for groundwater hydrodinamics analysis in a karst aquifer (Gran Sasso, Central Italy). Applied Geochemistry 20: 2063-2081.

Benjamin JR, Cornell CA (1960) Probability, statistics and decisions for civil engineering. McGraw-Hill, New York, 684 pp

Bonacci O (2007) Analysis of long-term (1878–2004) mean annual discharges of the karst spring Fontaine de Vaucluse (France). Acta Carsologica 36(1):151–156

Boni C, Bono P, Capelli G, 1986. Hydrogeological scheme of Central Italy. Mem. Soc. Geol. It. 35: 991–1012 (in Italian).

Brunetti MA, Maugeri M, Monti F, Nanni T (2006) Temperature and precipitation variability in Italy in the last two centuries from homogenised instrumental time series. Int J Climatol 26: 345–381

Celico P, Civita M (1976) Sulla tettonica del massiccio del Cervialto (Campania) e le implicazioni idrogeologiche ad essa connesse. Boll Soc Natur Naples 85:555–580

Calamita F, Di Domenica A, Viandante MG, Tavarnelli E (2008) Sovrascorrimenti younger on older o faglie normali ruotate: la linea Vallepietra-Filettino-Monte Ortara (Appennino centrale laziale-abruzzese). Rend. online SGI, 1 (2008), 43-47

Cavinato GP, De Celles PG 1999 Extensional basins in the tectonically bimodal central Apennines fold-thrust belt, Italy: response to corner flow above a subducting slab in retrograde motion. Geology 27: 955–958.

Civita M (1969) Idrogeologia del massiccio del Terminio-Tuoro (Campania). Memorie e Note Istituto di Geol Appl Univ di Napoli 11: 5–102

Caloiero T, Cosciarelli R, Ferrari E, Mancini M (2011) Precipitation change in Southern Italy linked to global scale oscillation index. Nat Hazard Earth Syst Sci 11:1683–1694

Desiderio G, Folchi Vici d'Arcevia C, Nanni T, Rusi S (2012) Hydrogeological mapping of the highly anthropogenically influenced Peligna Valley intramontane basin (Central Italy). Journal of Maps 8/2: 165-168. doi 10.1080/17445647.2012.680778

De Vita P, Allocca V, Manna F, and Fabbrocino S (2012) Coupled decadal variability of the North Atlantic Oscillation, regional rainfall and karst spring discharges in the Campania region (southern Italy), Hydrol. Earth Syst. Sci. 16: 1389–1399

Ducci D, Tranfaglia G (2008) Effects of climate change on groundwater resources in Campania (southern Italy). In: Special Publication. Climate change and groundwater vol. 288, Dragoni W, Sukhija BS (eds). Geological Society: London, 25-38

Fiorillo F, Esposito L, Guadagno FM (2007) Analyses and forecast of the water resource in an ultra-centenarian spring discharge series from Serino (Southern Italy) – Journal of Hydrology, 36: 125-138.

Fiorillo F. (2009) Spring hydrographs as indicators of droughts in a karst environment. Journal of Hydrology 373: 290-301.

Fiorillo F, Doglioni A (2010) The relation between karst spring discharge and rainfall by the cross-correlation analysis. Hydrogeology Journal 18: 1881-1895.

Fiorillo F, Guadagno FM (2010) Karst Spring Discharges Analysis in Relation to Drought Periods, Using the SPI. Water Resources Management 24: 1867-1884

Fiorillo F, Guadagno FM (2012) Long karst spring discharge time series and droughts occurrence in Southern Italy. Environmental Earth Sciences 65(8): 2273-2283.

Fiorillo F, Revellino P, Ventafridda G (2012) Karst aquifer drainage during dry periods. Journal of Cave and Karst Studies 74(2): 148–156.

Fiorillo F, Pagnozzi M, Ventafridda G (2014) A model to simulate recharge processes of karst massifs. Hydrological Processes (manuscript accepted).

Galassi DMP, Lombardo P, Fiasca B, Di Cioccio A, Di Lorenzo T, Petitta M, Di Carlo P (2014) Earthquake trigger the loss of groundwater biodiversità. Sci. Rep. 4, 6273 doi 10.1038/srep06273

Garbrecht J, Fernandez GP (1994) Visualization of trends and fluctuations in climatic records. Water Resour Bull 30(2): 297–306

Hurrell JW (1995) Decadal trends in the North Atlantic Oscillation: regional temperatures and precipitation. Science 269: 676 – 679.

Hurrell JW, Kushnir J, Ottersen G, Visbeck M. (2003) An Overview of the North Atlantic Oscillation. In "The North Atlantic Oscillation: Climatic Significance and Environmental Impact", Geophysical Monograph 134 Copyright 2003 by the American Geophysical Union 10.1029/134GM0

ISPRA (2009) Geological map of Italy, 1:50.000 scale. Istituto Superiore per la Protezione e la Ricerca Ambientale (ISPRA), Rome. http://www.apat.gov.it/Media/carg/

Lamb PJ, Peppler RA (1987) North Atlantic Oscillation: concept and an application. Bulletin of the American Meteorological Society 68(10): 1218 – 1225.

Lopez-Moreno JI, Vicente-Serrano SM (2008) Positive and negative Phases of the Winter-time North Atlantic Oscillation and Drought occurrence over Europe: multitemporal-scale approach, J. Climate 21: 1220–1241.

López-Moreno JI, Vicente-Serrano S.M., Morán-Tejeda E, Lorenzo-Lacruz J, Kenawy A, Beniston M (2011) Effects of the North Atlantic Oscillation (NAO) on combined temperature and

precipitation winter modes in the Mediterranean mountains: Observed relationships and projections for the 21st century. Global and Planetary Change 77: 62-76 doi 10.1016/j.gloplacha.2011.03.003

Magaldi D, Tallini M (2000) A micromorphological index of soil development for the Quaternary geology research. Catena 41: 261-276.

Massei N, Laignel B, Deloffre J, Mesquita J, Motelay A, Lafite R, Durand A (2009) Long-term hydrological changes of the Seine River flow (France) and their relation to the North Atlantic Oscillation over the period 1950 – 2008. International Journal of Climatology. doi 10.1002/joc.2022

Mecchia G, Mecchia M, Piro M, Barbati M (2003) Le grotte del Lazio. I fenomeni carsici, elementi della geodiversità. Edizion ARP. Available at http://www.parchilazio.it/home~nomepagina-pubblicazioni+id-55.htm, last accessed August 2014.

MOHC (2010) Global average temperature series 1850–2009. Met Office Hadley Centre (MOHC). http://www.metoffice.gov.uk/climatechange/science/hadleycentre/

Nanni T, Rusi S (2001) Correlation between the melting of the snows and the chemical-physical characteristics of springs, like parameter for the evaluation of karst aquifer vulnerability in Central Apennine. VII conference on Limestone Hydrology and fissured media. Besancon (France), 2001, Sci. Tech. Envir., Mem. H. S. 13: 261-264.

Nanni T, Rusi S (2003) Idrogeologia del massiccio carbonatico della Majella (Abruzzo) [Hydrogeology of the «Montagna della Majella» carbonate massif (Central Apennines-Italy)]. Boll. Soc. Geol. It. 122 (2): 173-202.

NCARS (National Center for Atmospheric Research Staff) Eds. Last modified 16 Apr 2014. "The Climate Data Guide: Hurrell North Atlantic Oscillation (NAO) Index (PC-based)." Retrieved from https://climatedataguide.ucar.edu/climate-data/hurrell-north-atlantic-oscillation-nao-index-pc-based. (last accessed July 2014)

Parotto M, Praturlon A (2004) The Southern Apennine Arc. In: Crescenti U, D'Offizi S, Merlino S, Sacchi L (eds). Special volume of the Italian Geological Society. 32nd International Geological Conference, Florence, pp 34–58.

Petitta M. 2009 hydrogeology of the middle valley of the Velino river and of the S. Vittorino plain (Rieti, central Italy). Italian Journal of Engineering Geology and Environment 1/2009, 157-182

Petitta M, Caschetto M, Galassi MPD, Aravena R (2014). Dual-flow in karst aquifers toward a steady discharge spring (Presciano, Central Italy): influences on a subsurface groundwater

dependent ecosystem and on changes related to post-earthquake hydrodynamics, Environmental Earth Sc, 10.1007/s12665-014-3440-1

Petitta M, Tallini M, (2002) Idrodinamica sotterranea del massiccio del Gran Sasso (Abruzzo): indagini idrologiche, idrogeologiche e idrochimiche (1994-2001). Boll Soc Geol It 121: 343-363.

Petitta M, Tallini M (2003) Groundwater resources and human impacts in a Quaternary intramontane basin (L'Aquila Plain, Central Italy). Water International 28: 57-69.

Preziosi E, Romano E (2013) Are large karstic springs good indicators for Climate Change effects on groundwater? Geophysical Research Abstracts 15, EGU2013-9367, 2013 EGU General Assembly 2013.

Romano E, Preziosi E (2013) Precipitation pattern analysis in the Tiber River basin (Central Italy) using standardized indices. Int. J. Climatol. 33: 1781–1792.

Romano E, Del Bon A, Petrangeli AB, Preziosi E (2013) Generating synthetic time series of springs discharge in relation to Standardized Precipitation Indices. Case study in Central Italy. Journal of Hydrology 507: 86–99.

Sani F., Del Ventisette C., Montanari D., Coli M., Nafissi P., Piazzini A. (2004) Tectonic evolution of the internal sector of the Central Apennines, Italy. Marine and Petroleum Geology 21: 1235–1254.

Scozzafava M, Tallini M (2001) Net infiltration in the Gran Sasso Massif (Central Italy): Thornthwaite water budget using the CN method (Soil Conservation Service). Hydrogeology Journal 9: 461-475.

Tallini M, Gasbarri D, Ranalli D, Scozzafava M (2006) Investigating the epikarst by low frequency GPR: an example from Gran Sasso range (Central Italy). Bulletin of Engineering Geology and the Environment 65: 435-443.

Tallini M, Parisse B, Petitta M, Spizzico M (2013) Long-term spatio-temporal hydrochemical and 222Rn tracing to investigate groundwater flow and water-rock interaction in the Gran Sasso (central Italy) carbonate aquifer. Hydrogeology Journal 21: 1447-1467. doi 10.1007/s10040-013-1023-y

Tallini M., Adinolfi Falcone R., Carucci V., Falgiani A., Parisse B., Petitta M. (2014) Isotope hydrology and geochemical modeling: new insights into recharge process and water-rock interaction in the Gran Sasso fissured carbonate aquifer (Central Italy). Environmental Earth Sciences. doi 10.1007/s12665-014-3364-9

Thornthwaite CW, Mather JR (1957) Instruction and tables for computing potential evapotranspiration and the water balance. Pubbl. Clim. Drexel Inst. Technol., 10.

Vicente-Serrano SM and Trigo, R. M. Eds. (2011) Hydrological, Socioeconomic and Ecological Impacts of the North Atlantic Oscillation in the Mediterranean Region (Advances in Global Change Research), Springer, 1–236.

Walker GT (1924) Correlation in seasonal variations of weather, IX. Memorandum of the India Meteorological Department 24: 275 – 332.

Walker GT, Bliss EW (1932) World Weather, VI Memorandum of the Royal Meteorological Society, Vol IV (36) 53 – 84.

Wang HF, Anderson MP (1982) Introduction to groundwater modeling: finite difference and finite element methods. Academic Press Inc. San Diego, California 92101-4495

Figures and tables

Fig. 1 Hydrogeological setting of the Latium-Abruzzi-Campania carbonate platform aquifers. 1 - Alluvial and coastal aquifer/aquitard systems; 2 - volcanic aquifers; 3 - fractured carbonate karstified aquifers; 4 - synorogenic and marls deposits (aquicludes); 5 - main thrust; 6 - main fault; 7 - main spring from carbonate aquifers (mean discharge > 1 m^3/s); 8 - main streambed spring (mean discharge > 1 m^3/s); 9 - studied monitored spring. Area A: Gran Sasso Aquifer; area B: Maiella aquifer; area C: Simbruini aquifer; area D: Picentini aquifer.

Fig. 2 Gran Sasso hydrogeological scheme (modified from Tallini et al., 2014). A – aquitard (continental detrital units, Quaternary); B – aquitard (terrigenous units, Mio-Pliocene); C – aquifer (carbonatic units of platform – reef included – and slope to basin lithofacies, Meso-Cenozoic; a: Gran Sasso aquifer, b: Sirente aquifer); D – low permeability substratum (dolomite, upper Triassic); E – overthrust T (no flow boundary); F – normal fault; G – main spring; H - studied springs of Tirino River Valley; I – streambed spring; J - groundwater flowpath; K – gauging station (TM: Tirino at Madonnina); L - highway tunnels and UL drainage (see Fig.1 for location).

Fig. 3 Occurrence of maximum and minimum monthly discharge values at Tirino Spring with long-term data.

Fig. 4 Hydrogeological sketch of Majella mountain (modified from Nanni and Rusi, 2003).
1) Slope breccias and debris, alluvial and lacustrine deposits (Quaternary); 2) argillaceous complex and flysch sequences (Paleogene–Pliocene); 3) calcareous-dolomite series (Jurassic–Miocene); 5) main karst spring; 6) Studied spring of Verde; 7) elevation (m a.s.l.); 8) village; 9) main endorheic area (see Fig.1 for location).

Fig. 5 Hydrogeological sketch of Simbruini Mountains. Main spring location and discharge (m^3/s), the triangle indicates a linear spring; 2: main thrust; 3: Travertine (Quaternary) ; 4: slope breccias and debris, alluvial and lacustrine deposits (Quaternary); 5: volcanic deposits (Quaternary); 6: Flysch (Miocene); 7: Calcareous formations (Trias sup. – Miocene); 8: Dolomite (Trias sup.) (see Fig.1 for location).

Fig. 6 Hydrogeological sketch of north-eastern sector of Picentini Mountains (modified from Fiorillo et al., 2014). 1) Slope breccias and debris, pyroclastic, alluvial and lacustrine deposits (Quaternary); 2) argillaceous complex and flysch sequences (Paleogene–Miocene); 3) calcareous-dolomite series (Jurassic–Miocene); 4) main karst spring; 5) village; 6)mountain peak; 7) elevation (m a.s.l.); 8) Spring catchment ; 9) endorheic area. (see Fig.1 for location).

Figure 7 a) Total monthly mean rainfall of rain gauges in Table 2; b) effective monthly mean rainfall computed by the Thornthwaite and Mather method (1957) for the same rain gauges.

Fig. 8 a) Monthly mean discharge of springs in Table 1; b) percentage variation of the monthly mean discharge for same springs.

Fig. 9 **a**) Standardized annual mean (November–October) karst spring discharge series, and NAO index PC-Based; **b**) standardized annual (September–August) rainfall series, and NAO index PC-Based (DJFM=December, January, February, March).

Fig. 10 a) Correlogram of the annual mean spring discharge series, and NAO PC-Based (data series in Table 4); b) Correlogram of the annual rainfall series, and NAO PC-Based (data series in Table 5).

Fig. 11 Rescaled adjust partial sums (RAPS). **a**) annual mean (November–October) spring discharge and NAO PC-based series; **b**) annual rainfall (September-August) and NAO index PC-based series.

Table 1 Main characteristics of karst springs analysed. μ, mean discharge; σ, standard deviation; Q_{90}, 90^{th} percentile; Q_{10}, 10^{th} percentile. *With some gaps.

Table 2 Characteristics of the rain gauges analysed. μ, annual mean rainfall (September-August); σ, standard deviation, μ_{summer}, summer mean rainfall (sum of June, July and August); μ_{autumn}, autumn mean rainfall (sum of September, October and November); μ_{winter}, winter mean rainfall (sum of December, January and February); μ_{spring}, spring mean rainfall (sum of March, April and May).

Table 3 Main hydrological parameters of springs and catchments (annual mean values); F, afflux on the massif; T, temperature; AET, actual evapotranspiration; R, recharge ($R=Q_s/F$). The mean, maximum and minimum values express the spatial variation of parameters.

Table 4 Correlation coefficients found between spring discharge time series, and NAO (data of Figure 9a); bold numbers mean a significance level, $\alpha<0.05$.

Table 5 - Correlation coefficients found between annual rainfall time series, and NAO (data of Figure 9b); bold numbers mean a significance level, $\alpha<0.05$.

Table 6 Correlation coefficients found of annual rainfall vs spring discharge time series (data of Figures 9 a-b); bold numbers mean a significance level, $\alpha<0.05$.

Table 7 Correlation coefficients found between annual mean spring discharge and NAO, for different moving average of time series.

Table 8 Correlation coefficients found between annual rainfall and NAO, for different moving average of time series.

Figure

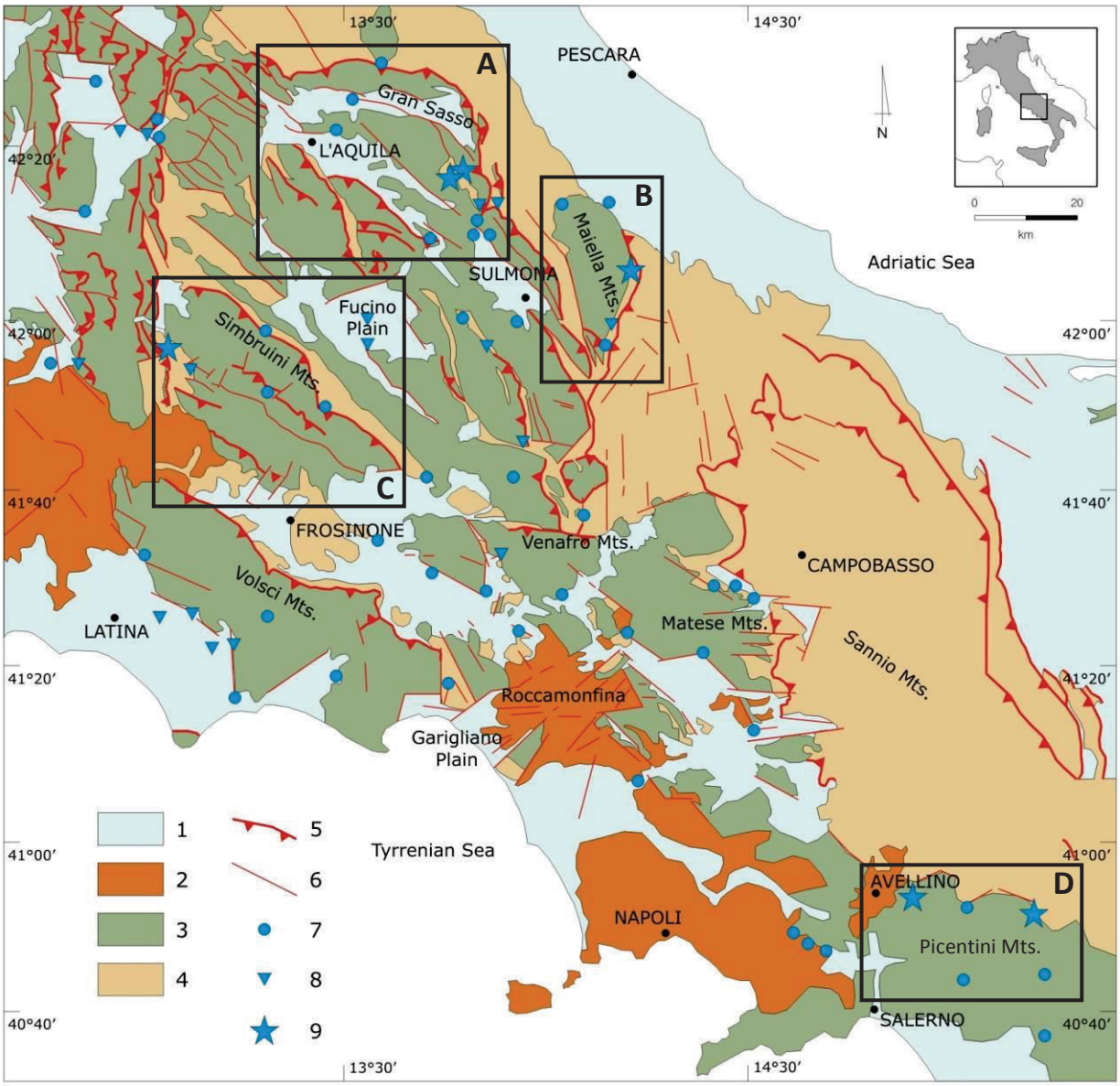

Fig. 1 Hydrogeological setting of the Latium-Abruzzi-Campania carbonate platform aquifers. 1 - Alluvial and coastal aquifer/aquitard systems; 2 - volcanic aquifers; 3 - fractured carbonate karstified aquifers; 4 - synorogenic and marls deposits (aquicludes); 5 - main thrust; 6 - main fault; 7 - main spring from carbonate aquifers (mean discharge > 1 m^3/s); 8 - main streambed spring (mean discharge > 1 m^3/s); 9 - studied monitored spring. Area A: Gran Sasso Aquifer; area B: Maiella aquifer; area C: Simbruini aquifer; area D: Picentini aquifer.

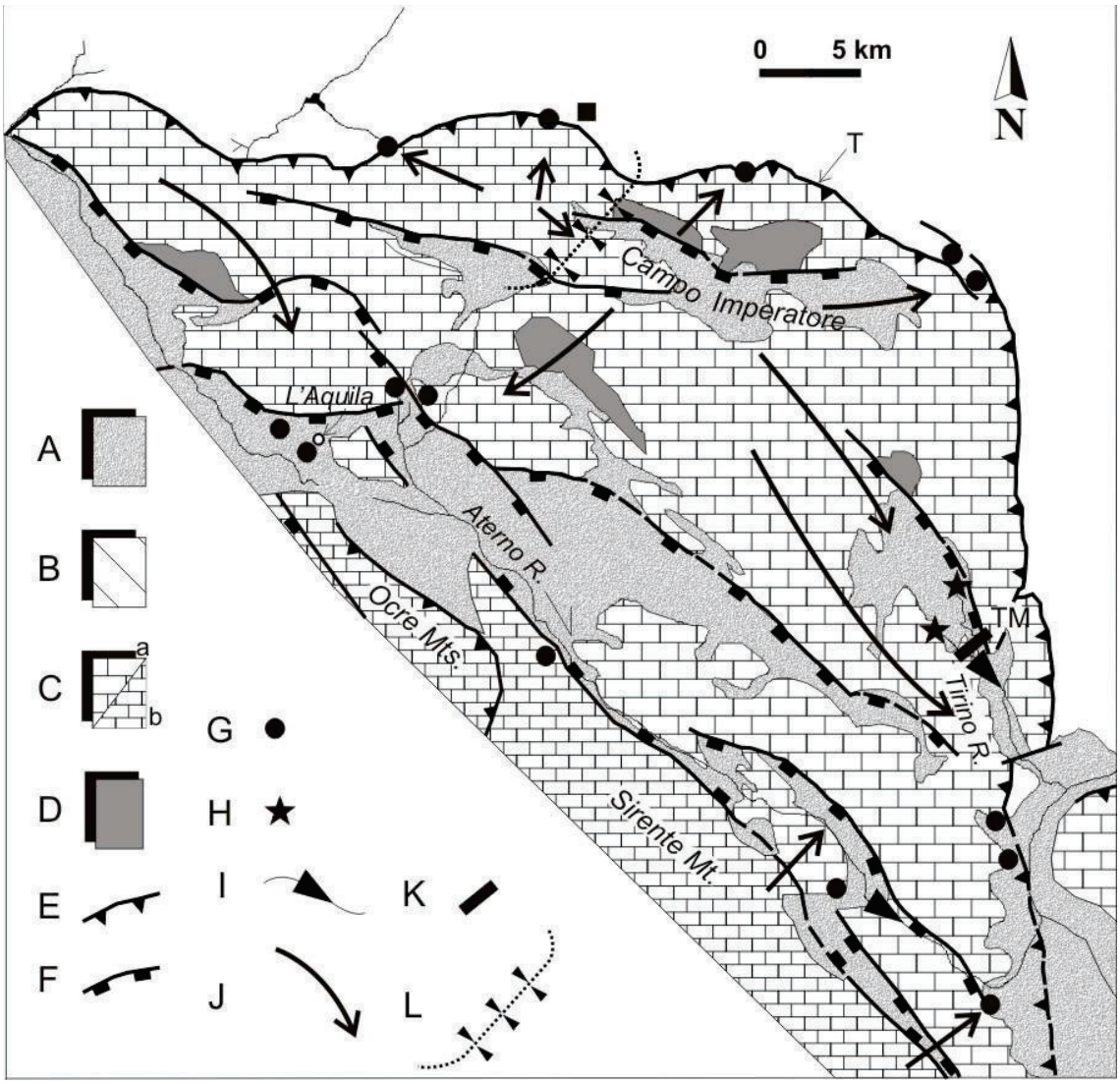

Fig. 2 Gran Sasso hydrogeological scheme (modified from Tallini et al., 2014). A – aquitard (continental detrital units, Quaternary); B – aquitard (terrigenous units, Mio-Pliocene); C – aquifer (carbonatic units of platform – reef included – and slope to basin lithofacies, Meso-Cenozoic; a: Gran Sasso aquifer, b: Sirente aquifer); D – low permeability substratum (dolomite, upper Triassic); E – overthrust T (no flow boundary); F – normal fault; G – main spring; H - studied springs of Tirino River Valley; I – streambed spring; J - groundwater flowpath; K – gauging station (TM: Tirino at Madonnina); L - highway tunnels and UL drainage (see Fig.1 for location).

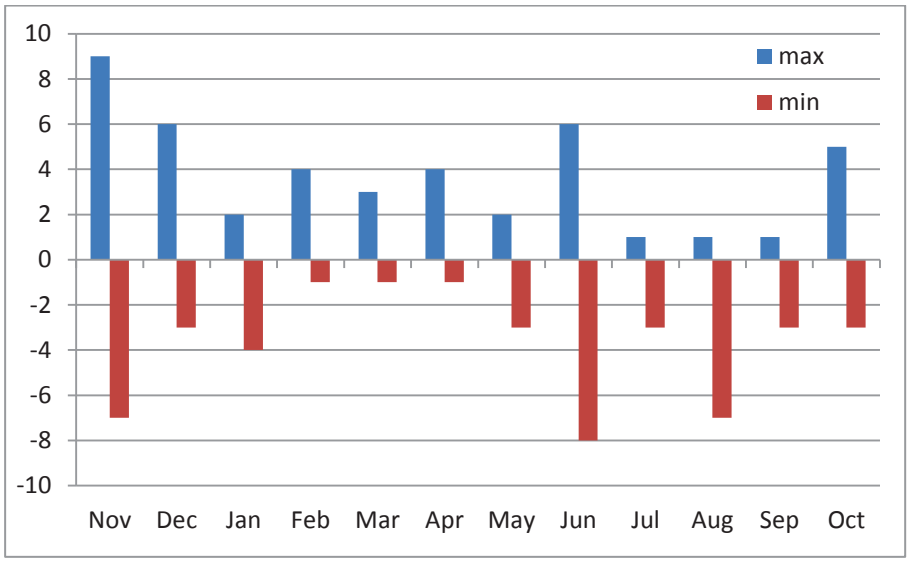

Fig. 3 Occurrence of maximum and minimum monthly discharge values at Tirino Spring with long-term data.

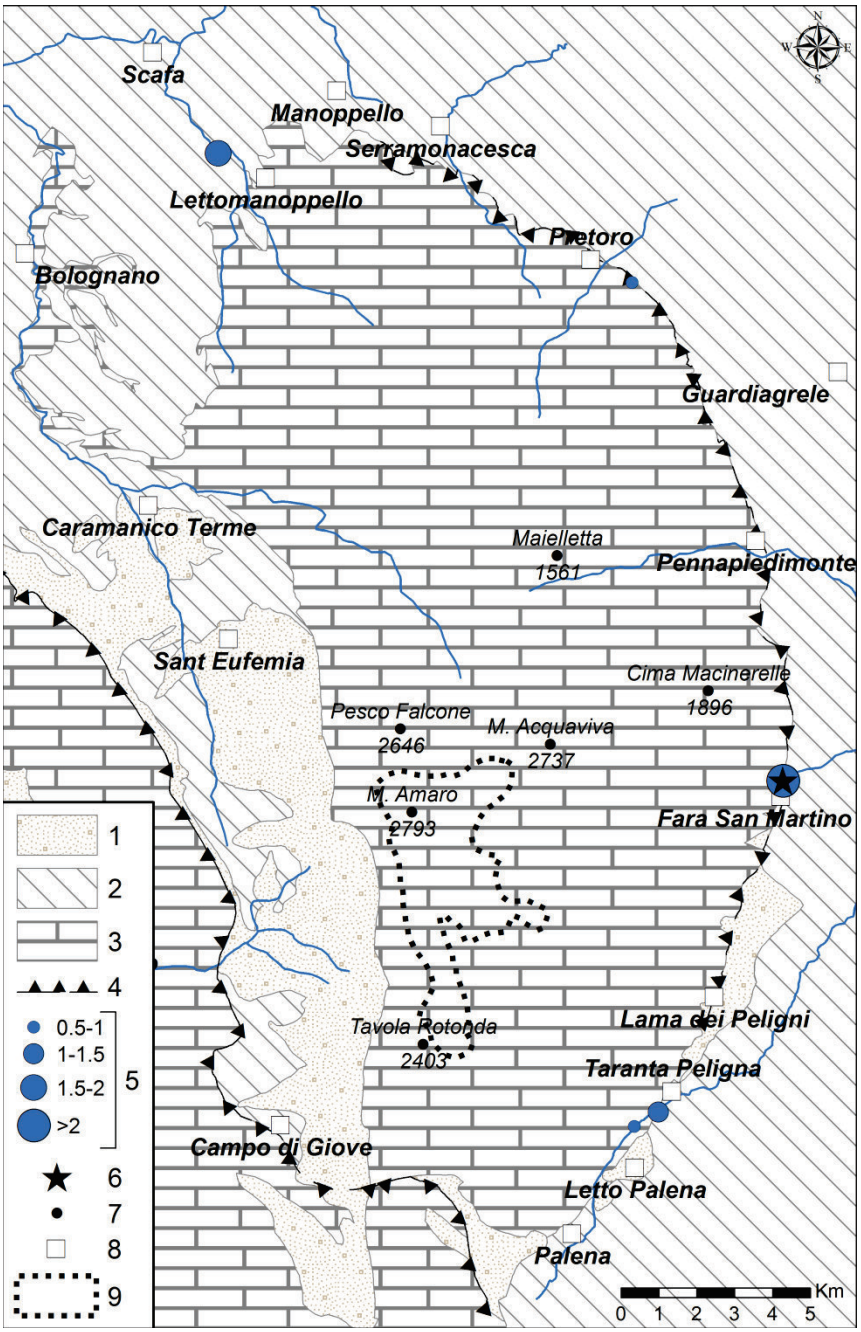

Fig. 4 Hydrogeological sketch of Majella mountain (modified from Nanni and Rusi, 2003).

1) Slope breccias and debris, alluvial and lacustrine deposits (Quaternary); 2) argillaceous complex and flysch sequences (Paleogene–Pliocene); 3) calcareous-dolomite series (Jurassic–Miocene); 5) main karst spring; 6) Studied spring of Verde; 7) elevation (m a.s.l.); 8) village; 9) main endorheic area (see Fig.1 for location).

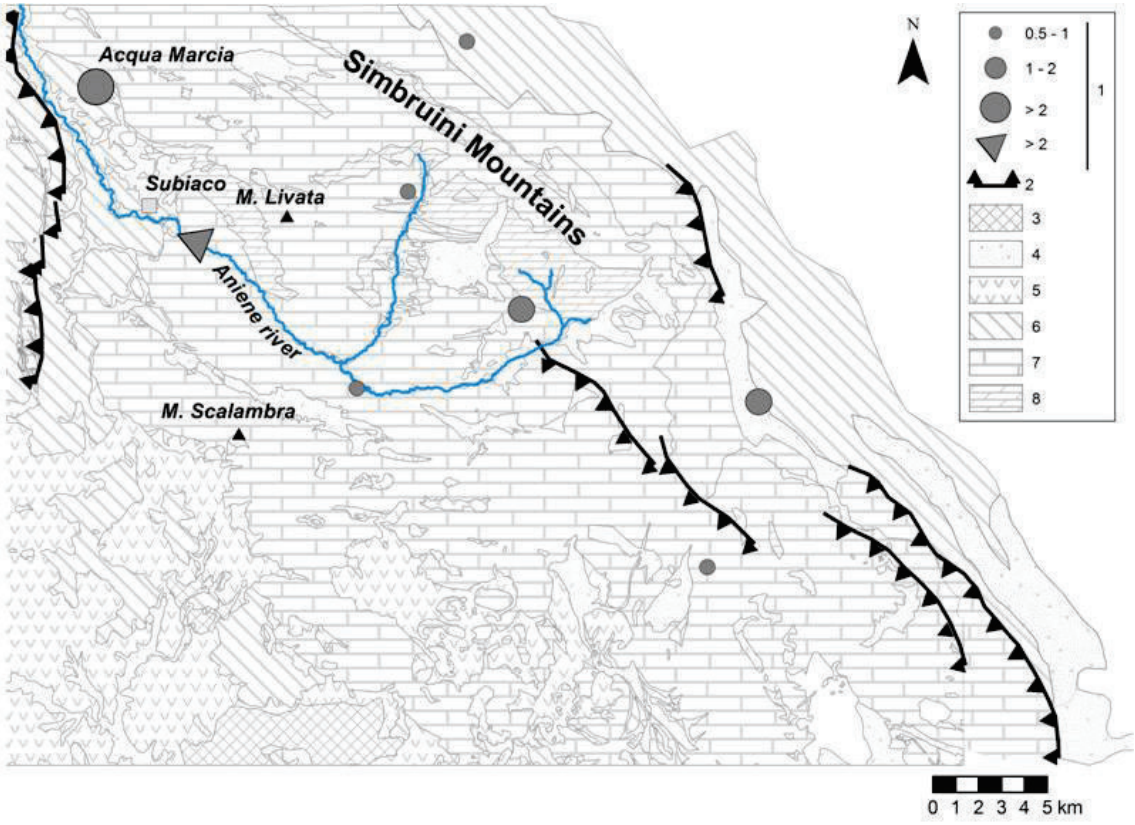

Fig. 5 Hydrogeological sketch of Simbruini Mountains.

Main spring location and discharge (m^3/s), the triangle indicates a linear spring; 2: main thrust; 3: Travertine (Quaternary) ; 4: slope breccias and debris, alluvial and lacustrine deposits (Quaternary); 5: volcanic deposits (Quaternary); 6: Flysch (Miocene); 7: Calcareous formations (Trias sup. – Miocene); 8: Dolomite (Trias sup.) (see Fig.1 for location)

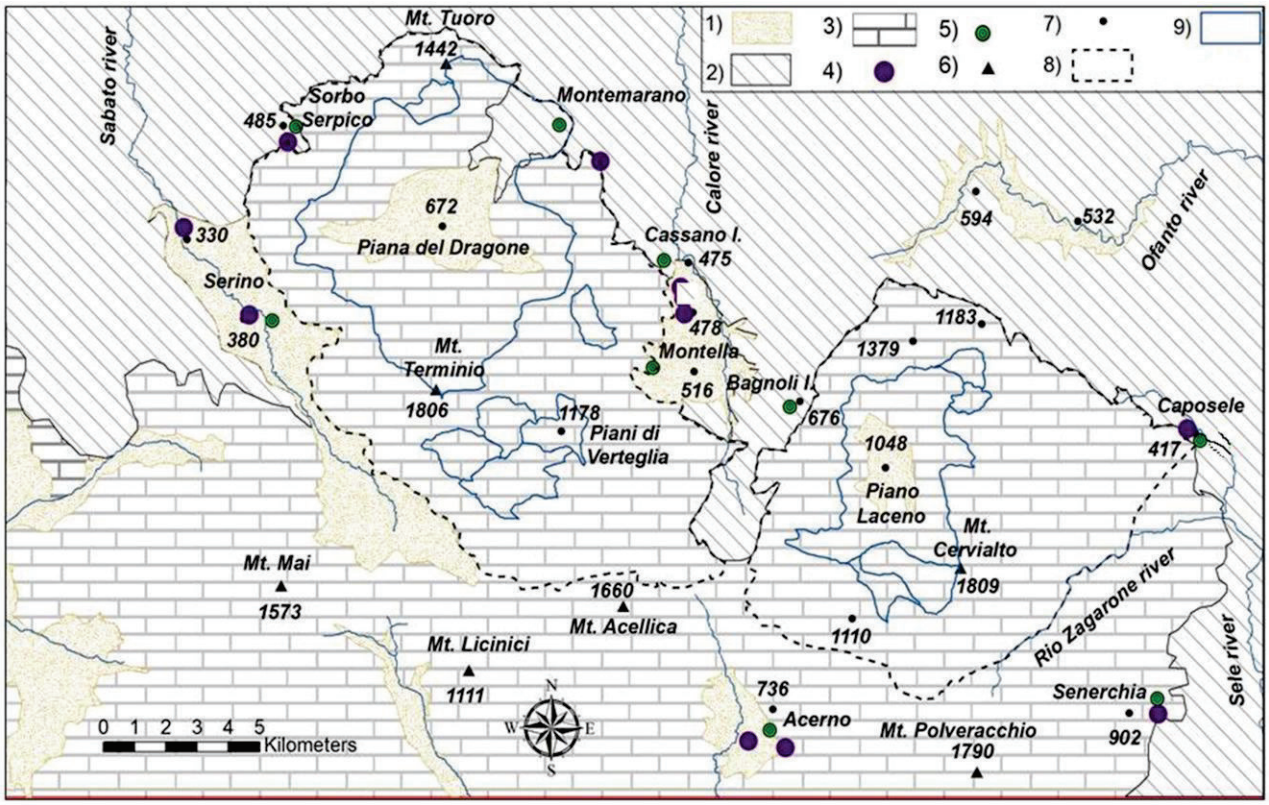

Fig. 6 Hydrogeological sketch of north-eastern sector of Picentini Mountains (modified from Fiorillo et al., 2014). 1) Slope breccias and debris, pyroclastic, alluvial and lacustrine deposits (Quaternary); 2) argillaceous complex and flysch sequences (Paleogene–Miocene); 3) calcareous-dolomite series (Jurassic–Miocene); 4) main karst spring; 5) village; 6)mountain peak; 7) elevation (m a.s.l.); 8) Spring catchment ; 9) endorheic area. (see Fig.1 for location).

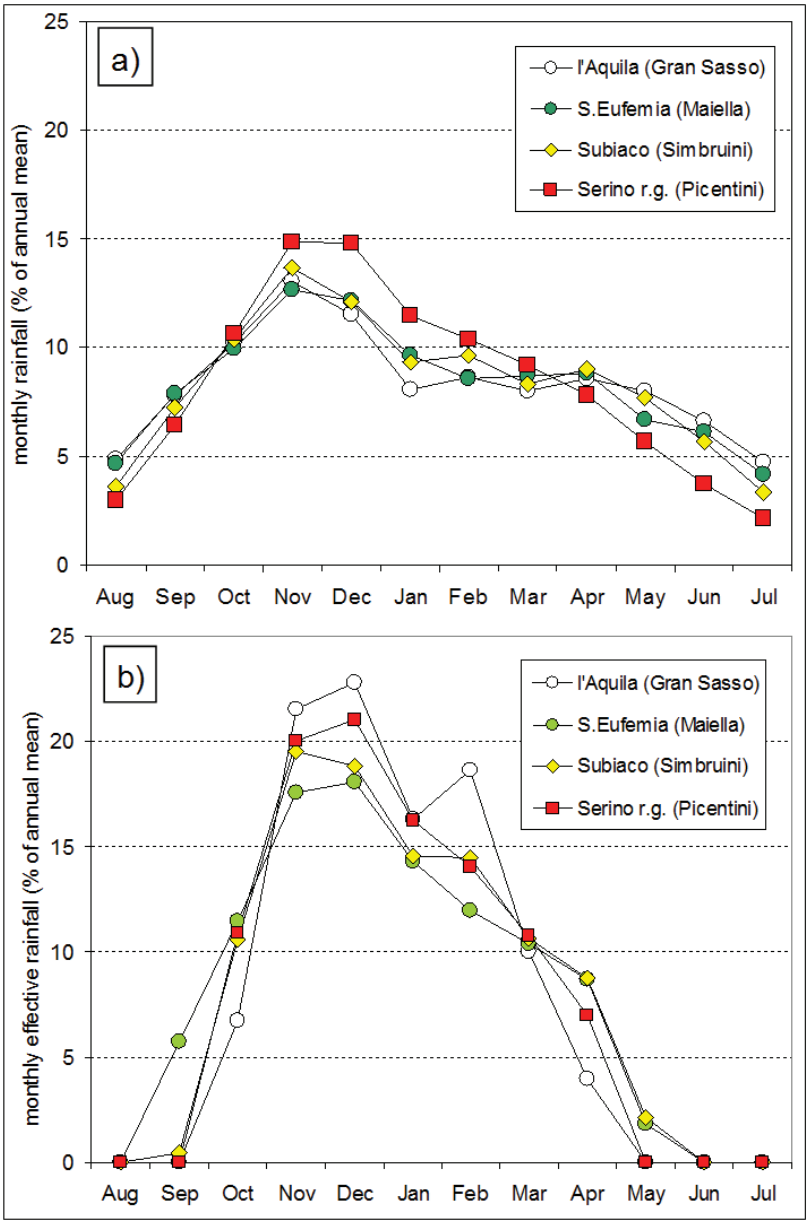

Figure 7 a) Total monthly mean rainfall of rain gauges in Table 2; b) effective monthly mean rainfall computed by the Thornthwaite and Mather method (1957) for the same rain gauges.

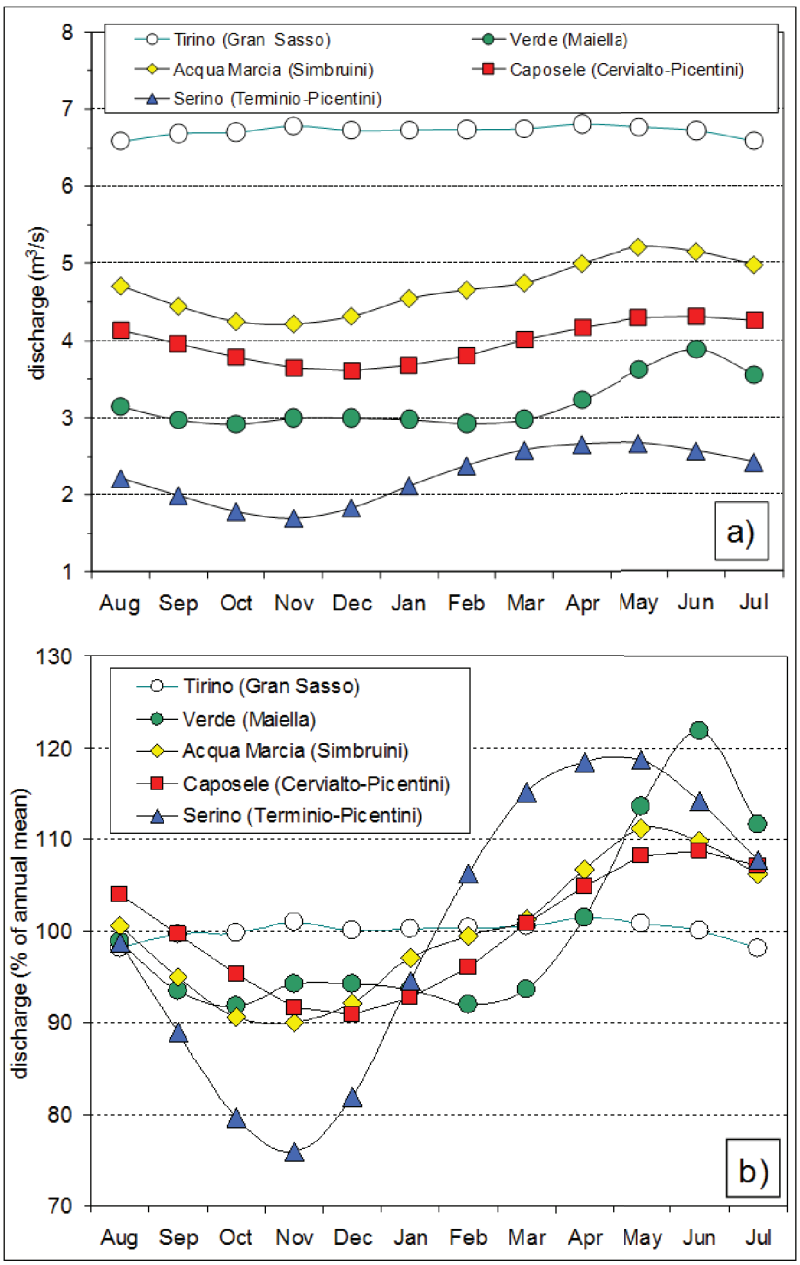

Figure 8 a) Monthly mean discharge of springs in Table 1; b) percentage variation of the monthly mean discharge for same springs.

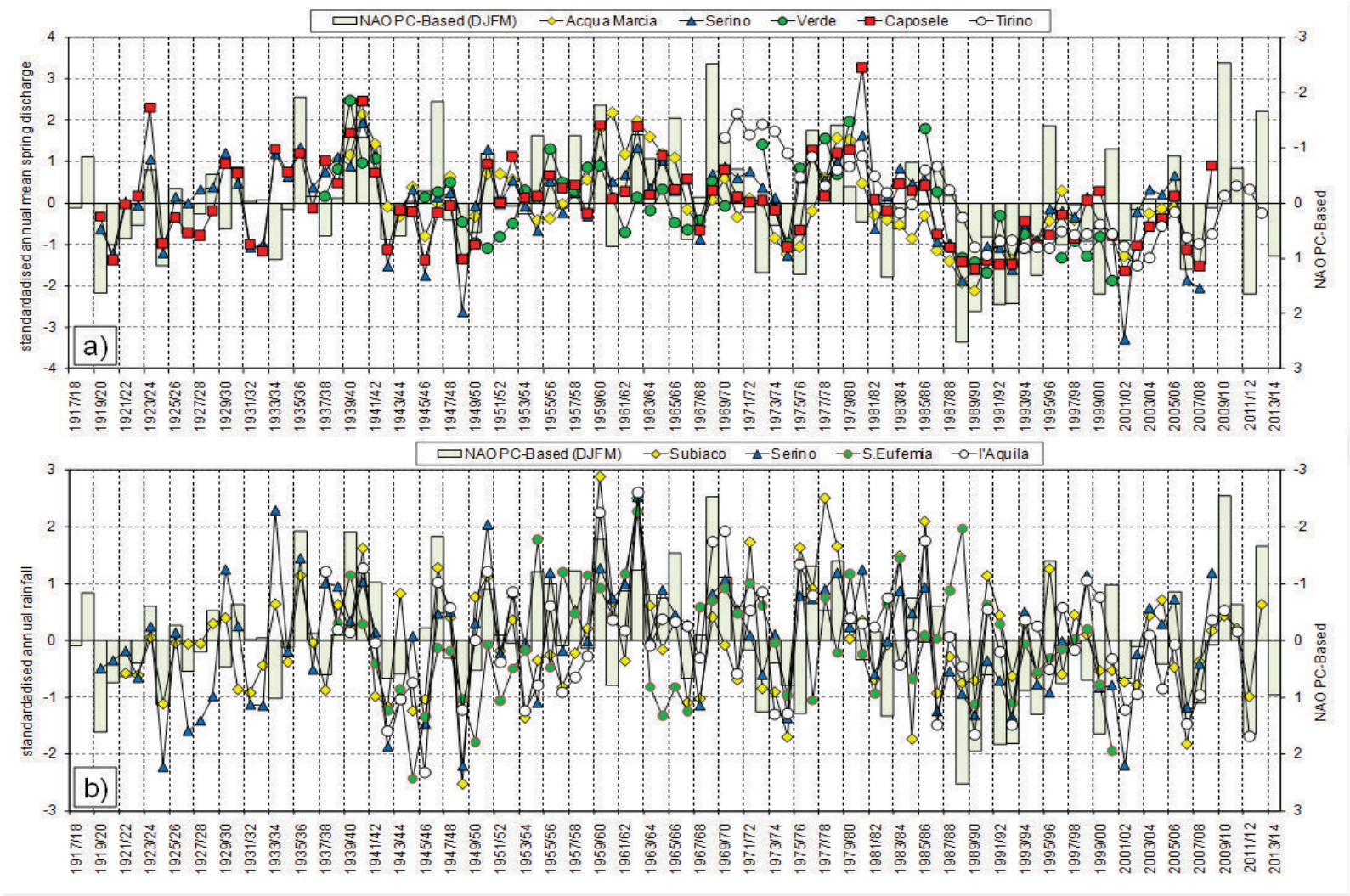

Figure 9 **a**) Standardized annual mean (November–October) karst spring discharge series, and NAO index PC-Based; **b**) standardized annual (September–August) rainfall series, and NAO index PC-Based (DJFM=December, January, February, March).

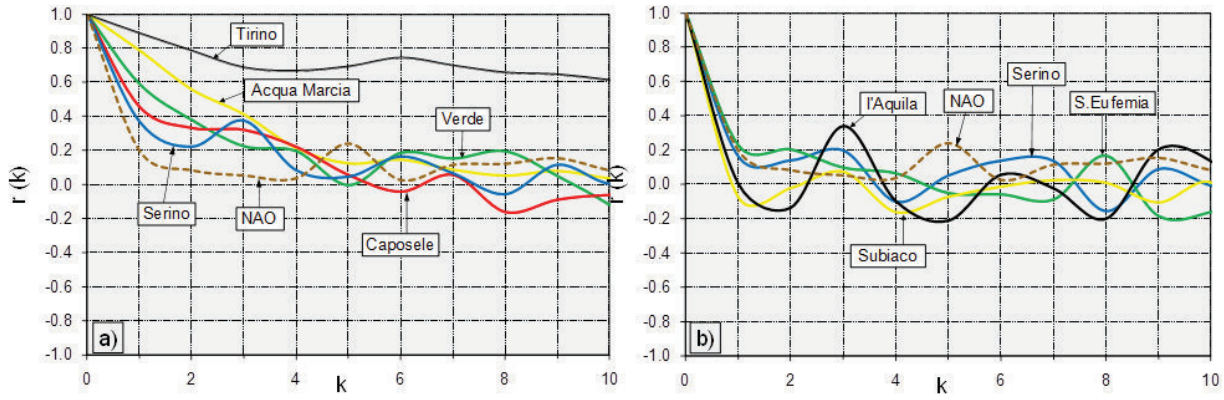

Fig 10 a) Correlogram of the annual mean spring discharge series, and NAO PC-Based (data series in Table 4); b) Correlogram of the annual rainfall series, and NAO PC-Based (data series in Table 5).

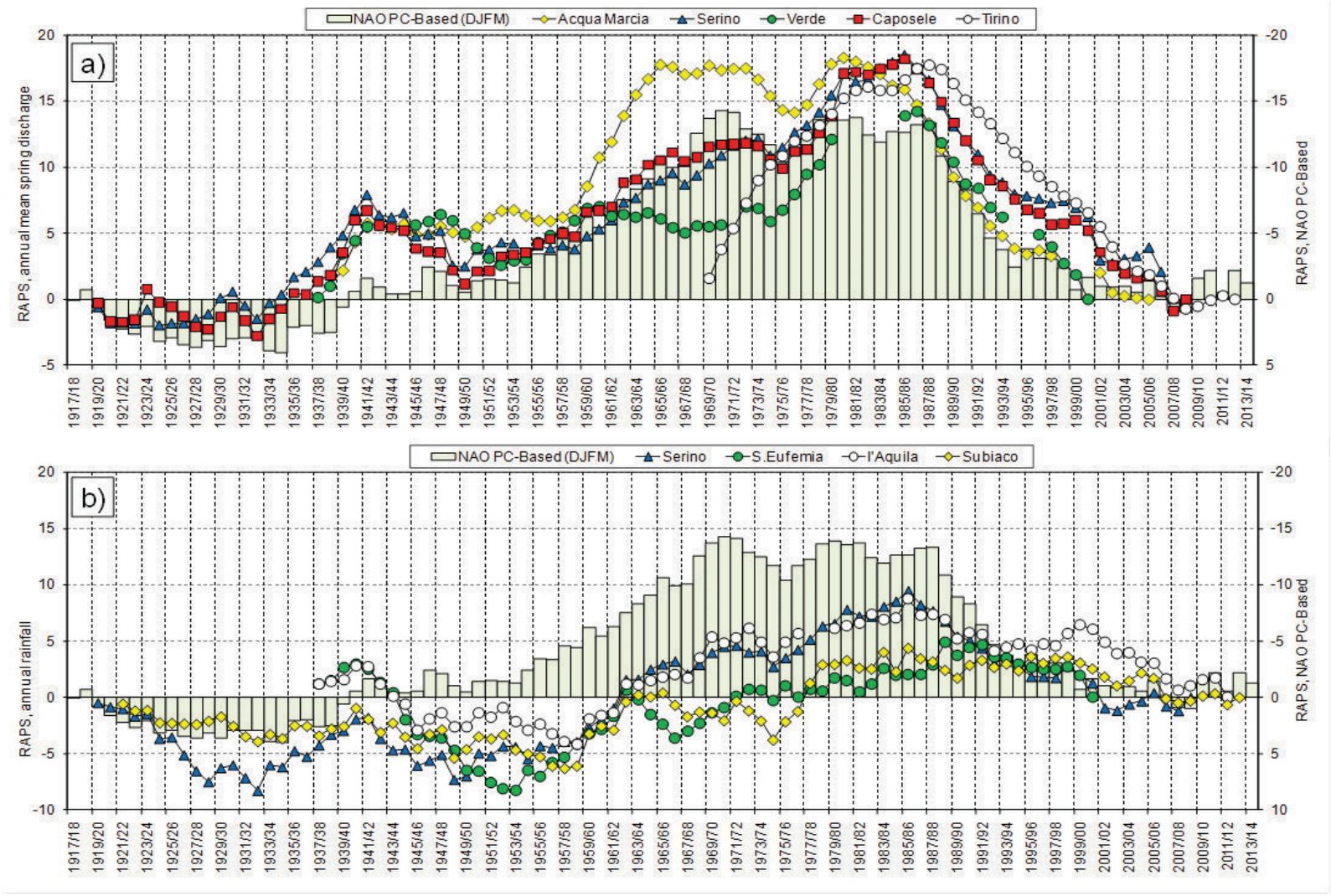

Figure 11 Rescaled adjust partial sums (RAPS). **a**) annual mean (November–October) spring discharge and NAO PC-based series; **b**) annual rainfall (September-August) and NAO index PC-based series

Table

Table 1. Main characteristics of karst springs analysed. μ, mean discharge; σ, standard deviation; Q_{90}, 90th percentile; Q_{10}, 10th percentile. *With some gaps.

Catchment	**Gran Sasso**	**Maiella**	**Simbruini**	**Picentini**	
Spring name	Tirino	Verde	Acqua Marcia	Caposele	Serino
Elevation (m a.s.l.)	310-340	410	322-329 m	417	330-380
Time interval of data series	Jan 1970 Dec 2013	Jan 1938 Dec 2001*	Jan 1938 March 2007*	Jan 1920 Dec 2009	Jan 1887 Dec 2008
μ *(m^3/s)*	6.76	3.19	4.8	3.96	2.24
σ *(m^3/s)*	1.70	0.58	1.09	0.59	0.33
Q_{90} *(m^3/s)*	9.1	3.97	6.32	4.89	2.64
Q_{10} *(m^3/s)*	5.0	2.54	3.48	3.14	1.81

Table 2. Characteristics of the rain gauges analysed. μ, annual mean rainfall (September-August); σ, standard deviation, μ_{summer}, summer mean rainfall (sum of June, July and August); μ_{autumn}, autumn mean rainfall (sum of September, October and November); μ_{winter}, winter mean rainfall (sum of December, January and February); μ_{spring}, spring mean rainfall (sum of March, April and May).

Catchment	**Gran Sasso**	**Majella**	**Simbruini**	**Picentini**
Rain gauge	L'Aquila	S. Eufemia	Subiaco Santa Scolastica	Serino
Elevation (m a.s.l.)	735	870	952	351
Time interval of data series	1938 - 2012	1938 - 2001	1921-2013	1920 - 2009
μ *(mm)*	684	1410	1197	1334
σ *(mm)*	142	268	246	283
μ_{summer} *(mm)*	115	211	170	117
μ_{autumn} *(mm)*	221	430	433	426
μ_{winter} *(mm)*	201	426	326	489
μ_{spring} *(mm)*	175	340	268	300

Table 3 Main hydrological parameters of springs and catchments (annual mean values); F, afflux on the massif; T, temperature; AET, actual evapotranspiration; R, recharge ($R=Q_s/F$). The mean, maximum and minimum values express the spatial variation of parameters

Spring group and discharge, Q_s (m^3/s)		**Catchment, main features**		**mean**	**max**	**min**	***F*** ($m^3\times10^6/y$)	***R*** **(%)**
Serino	2.25	Terminio					334.3	50.1
Cassano I.	2.65		*F*, (mm/y)	1887	2547	1463		
Sorbo Serp.	0.43		*T*, (°C)	10.3	15.5	4.4		
Others	0.15		*AET* (mm)	587	703	413		
Total output	**5.48**							
Caposele	4.00	Cervialto	*F*, (mm/y)	2109	2620	1529	238.8	54.3
Others	0.17		*T*, (°C)	8.5	14.0	4.4		
Total output	**4.17**		*AET*, (mm)	529	688	410		

Table 4 Correlation coefficients found between spring discharge time series, and NAO (data of Figure 9a); bold numbers mean a significance level, $\alpha<0.05$.

	Serino	**Caposele**	**Verde**	**Acqua Marcia**	**Tirino**
Caposele	**0.85**	-	-	-	-
Verde	**0.57**	**0.59**	-	-	-
Acqua Marcia	**0.70**	**0.75**	**0.47**	-	-
Tirino	**0.54**	**0.54**	**0.66**	**0.44**	-
NAO PC-Based	**-0.53**	**-0.51**	**-0.44**	**-0.55**	-0.27

Table 5 - Correlation coefficients found between annual rainfall time series, and NAO (data of Figure 9b); bold numbers mean a significance level, $\alpha<0.05$.

	Serino	**S.Eufemia**	**Subiaco**	**l'Aquila**
S.Eufemia	**0.33**	-	-	-
Subiaco	**0.59**	**0.36**	-	-
l'Aquila	**0.74**	**0.39**	**0.64**	-
NAO PC-Based	**-0.42**	-0.08	**-0.36**	**-0.37**

Table 6 - Correlation coefficients found of annual rainfall vs spring discharge time series (data of Figures 9 a-b); bold numbers mean a significance level, $\alpha<0.05$.

	Serino (spring)	Caposele	Verde	Acqua Marcia	Tirino
Serino (rain gauge)	**0.81**	**0.73**	**0.35**	**0.61**	**0.31**
S.Eufemia	0.25	0.24	**0.33**	0.12	0.24
Subiaco	**0.53**	**0.40**	**0.32**	**0.41**	0.06
l'Aquila	**0.66**	**0.60**	0.27	**0.50**	0.25

Table 7 Correlation coefficients found between annual mean spring discharge and NAO, for different moving average of time series

	Serino	Caposele	Verde	Acqua Marcia	Tirino
2-yrs mov.average	-0.62	-0.62	-0.57	-0.66	-0.40
5-yrs mov.average	-0.75	-0.76	-0.54	-0.80	-0.58
11-yrs mov.average	-0.81	-0.85	-0.76	-0.96	-0.49

Table 8 Correlation coefficients found between annual rainfall and NAO, for different moving average of time series

	Serino	S.Eufemia	Subiaco	l'Aquila
2-yrs mov.average	-0.52	-0.18	-0.40	-0.44
5-yrs mov.average	-0.68	-0.19	-0.32	-0.48
11-yrs mov.average	-0.80	-0.15	-0.35	-0.57